

Basic Study

Evaluation of biodegradable electric conductive tube-guides and mesenchymal stem cells

Jorge Ribeiro, Tiago Pereira, Ana Rita Caseiro, Paulo Armada-da-Silva, Isabel Pires, Justina Prada, Irina Amorim, Sandra Amado, Miguel França, Carolina Gonçalves, Maria Ascensão Lopes, José Domingos Santos, Dina Morais Silva, Stefano Geuna, Ana Lúcia Luís, Ana Colette Maurício

Jorge Ribeiro, Tiago Pereira, Ana Rita Caseiro, Miguel França, Ana Lúcia Luís, Ana Colette Maurício, Departamento de Clínicas Veterinárias and [†]UPVet, Instituto de Ciências Biomédicas de Abel Salazar (ICBAS) and Centro de Estudos de Ciência Animal (CECA), Instituto de Ciências, Tecnologia e Agroambiente da Universidade do Porto (ICETA), Rua de Jorge Viterbo Ferreira, 4050-313 Porto, Portugal

Paulo Armada-da-Silva, Sandra Amado, Centro Interdisciplinar de Estudo de Performance Humana (CIPER), Faculdade de Motricidade Humana (FMH), Universidade de Lisboa (UL), Estrada da Costa, 1499-002 Cruz Quebrada, Dafundo, Portugal

Isabel Pires, Justina Prada, CECAV and Departamento de Ciências Veterinárias, Universidade de Trás-os-Montes e Alto Douro (UTAD), 5001-801 Vila Real, Portugal

Irina Amorim, Departamento de Patologia e de Imunologia Molecular, Instituto de Ciências Biomédicas de Abel Salazar, Rua de Jorge Viterbo Ferreira, 4050-313 Porto, Portugal

Irina Amorim, Instituto Português de Patologia e Imunologia Molecular da Universidade do Porto (IPATIMUP), Rua Dr. Roberto Frias s/n, 4200-465 Porto, Portugal

Sandra Amado, UIS-IPL: Unidade de Investigação em Saúde da Escola Superior de Saúde de Leiria, Instituto Politécnico de Leiria, 2411-901 Leiria, Portugal

Carolina Gonçalves, Maria Ascensão Lopes, José Domingos Santos, CEMUC, Departamento de Engenharia Metalúrgica e Materiais, Faculdade de Engenharia da Universidade do Porto (FEUP), Rua Dr. Roberto Frias, 4200-465 Porto, Portugal

Dina Morais Silva, Biosskin, Molecular and Cell Therapies S.A. TecMaia, Rua Engenheiro Frederico Ulrich 2650, 4470-605 Maia, Portugal

Stefano Geuna, Neuroscience Institute of the Cavalieri Ottolenghi Foundation and Department of Clinical and Biological Sciences, University of Turin, 10124 Turin, Italy

Author contributions: Ribeiro J and Pereira T equally contributed; all authors contributed to this manuscript.

Supported by System of Incentives for Research and Technological development of QREN in the scope of project n° 38853/2013 - DEXGENERATION: “Soluções avançadas de regeneração óssea com base em hidrogéis de dextrin”; by the European Community FEDER fund through ON2 - O Novo Norte - North Portugal Regional Operational Program 2007-2013; by Project n° 34128 - BEPIM II: “Microdispositivos biomédicos com capacidade osteointegrativa por μ PIM”; funded by AdI, and by the program COMPETE - Programa Operacional Factores de Competitividade, projects Pest-OE/AGR/UI0211/2011; PTDC/CVT/103081/2008; and CDRsp’s Strategic Project - UI-4044-2011-2012 (Pest-OE/EME/UI4044/2011) funding from FCT.

Institutional review board statement: The article describes a basic research study involving animal subjects and was reviewed and approved by the Instituto de Ciências Biomédicas Abel Salazar (ICBAS) - University of Porto (UP) and CECA-ICETA scientific boards. All procedures involving the experimental animals were performed with the approval of the Veterinary Authorities of Portugal in accordance with the European Communities Council Directive of November 1986 (86/609/EEC), and the NIH guidelines for the care and use of laboratory animals have been observed.

Institutional animal care and use committee statement: The article describes a basic research study involving animal subjects and was approved by the Veterinary Authorities of Portugal in accordance with the European Communities Council Directive of November 1986 (86/609/EEC), and the NIH guidelines for the care and use of laboratory animals have been observed. Also all the authors involved in the *in vivo* tasks have a degree in Veterinary Medicine and are accredited by the Veterinary Authorities of Portugal (Direcção Geral de Alimentação e Veterinária - DGAV) and by Felasa - Category C for working with laboratory animals. Humane end points were always followed in accordance to the OECD Guidance Document on the Recognition, Assessment and Use of Clinical Signs as Humane Endpoints for Experimental Animals Used in Safety Evaluation (2000).

Adequate measures were taken to minimize pain and discomfort taking into account human endpoints for animal suffering and distress. Animals were housed for two weeks before entering the experiment.

Conflict-of-interest statement: The authors state that they do not have any conflict of interests, including commercial, personal, political, intellectual, or religious interests that are related to the work submitted for consideration of publication.

Data sharing statement: This work is original in that it has not been published before or submitted for publication elsewhere, and will not be submitted elsewhere before a decision has been taken as to its acceptability in this Journal where you are Editor. Each author meets the criteria for authorship and assumes the corresponding responsibility. Technical appendix, statistical code, and dataset available from the corresponding author at Dryad repository, who will provide a permanent, citable and open-access home for the dataset is provided.

Open-Access: This article is an open-access article which was selected by an in-house editor and fully peer-reviewed by external reviewers. It is distributed in accordance with the Creative Commons Attribution Non Commercial (CC BY-NC 4.0) license, which permits others to distribute, remix, adapt, build upon this work non-commercially, and license their derivative works on different terms, provided the original work is properly cited and the use is non-commercial. See: <http://creativecommons.org/licenses/by-nc/4.0/>

Correspondence to: Ana Colette Maurício, Professor, Departamento de Clínicas Veterinárias and +UPVet, Instituto de Ciências Biomédicas de Abel Salazar (ICBAS) and Centro de Estudos de Ciência Animal (CECA), Instituto de Ciências, Tecnologias e Agroambiente da Universidade do Porto (ICETA), Rua de Jorge Viterbo Ferreira, n° 228, 4050-313 Porto, Portugal. ana.colette@hotmail.com
Telephone: +351-220-428000

Received: February 2, 2015

Peer-review started: February 2, 2015

First decision: March 6, 2015

Revised: April 17, 2015

Accepted: May 5, 2015

Article in press: May 6, 2015

Published online: July 26, 2015

Abstract

AIM: To study the therapeutic effect of three tube-guides with electrical conductivity associated to mesenchymal stem cells (MSCs) on neuro-muscular regeneration after neurotmesis.

METHODS: Rats with 10-mm gap nerve injury were tested using polyvinyl alcohol (PVA), PVA-carbon nanotubes (CNTs) and MSCs, and PVA-polypyrrole (PPy). The regenerated nerves and tibialis anterior muscles were processed for stereological studies after 20 wk. The functional recovery was assessed serially for gait biomechanical analysis, by extensor postural thrust, sciatic functional index and static sciatic functional

index (SSI), and by withdrawal reflex latency (WRL). *In vitro* studies included cytocompatibility, flow cytometry, reverse transcriptase polymerase chain reaction and karyotype analysis of the MSCs. Histopathology of lung, liver, kidneys, and regional lymph nodes ensured the biomaterials biocompatibility.

RESULTS: SSI remained negative throughout and independently from treatment. Differences between treated groups in the severity of changes in WRL existed, showing a faster regeneration for PVA-CNTs-MSCs ($P < 0.05$). At toe-off, less acute ankle joint angles were seen for PVA-CNTs-MSCs group ($P = 0.051$) suggesting improved ankle muscles function during the push off phase of the gait cycle. In PVA-PPy and PVA-CNTs groups, there was a 25% and 42% increase of average fiber area and a 13% and 21% increase of the "minimal Feret's diameter" respectively. Stereological analysis disclosed a significantly ($P < 0.05$) increased myelin thickness (M), ratio myelin thickness/axon diameter (M/d) and ratio axon diameter/fiber diameter (d/D; g-ratio) in PVA-CNT-MSCs group ($P < 0.05$).

CONCLUSION: Results revealed that treatment with MSCs and PVA-CNTs tube-guides induced better nerve fiber regeneration. Functional and kinematics analysis revealed positive synergistic effects brought by MSCs and PVA-CNTs. The PVA-CNTs and PVA-PPy are promising scaffolds with electric conductive properties, bio- and cytocompatible that might prevent the secondary neurogenic muscular atrophy by improving the reestablishment of the neuro-muscular junction.

Key words: Nerve regeneration; Neurotmesis; Tube-guides; Mesenchymal stem cells; Carbon nanotubes; Functional assessment; Gait biomechanical analysis; Histomorfometry; Polyvinyl alcohol

© The Author(s) 2015. Published by Baishideng Publishing Group Inc. All rights reserved.

Core tip: The rat sciatic injury neurotmesis injury model is an appropriate model to evaluate the nerve regeneration when electric conductive tube-guides of polyvinyl alcohol (PVA)-carbon nanotubes (CNTs) and PVA-polypyrrole (PPy) associated to mesenchymal stem cells (MSCs) are used as scaffolds. The results obtained revealed that treatment with MSCs associated to PVA-CNTs tube-guides induced an increased number of regenerated fibers and thickening of the myelin sheet. Functional and kinematics analysis revealed positive synergistic effects brought by MSCs and PVA-CNTs. The PVA-CNTs and PVA-PPy are promising scaffolds with electric conductive properties, bio- and cytocompatible that might prevent the secondary neurogenic muscular atrophy by improving the reestablishment of the neuro-muscular junction.

Ribeiro J, Pereira T, Caseiro AR, Armada-da-Silva P, Pires I, Prada J, Amorim I, Amado S, França M, Gonçalves C, Lopes

MA, Santos JD, Silva DM, Geuna S, Luís AL, Maurício AC. Evaluation of biodegradable electric conductive tube-guides and mesenchymal stem cells. *World J Stem Cells* 2015; 7(6): 956-975 Available from: URL: <http://www.wjgnet.com/1948-0210/full/v7/i6/956.htm> DOI: <http://dx.doi.org/10.4252/wjsc.v7.i6.956>

INTRODUCTION

Functional recovery is rarely satisfactory in patients where peripheral nerve repair is needed, remaining a challenging task in neurosurgery^[1,2]. Direct repair is the procedure of choice but only when a tension-free end-to-end suture is possible. However, for patients with loss of nerve tissue, resulting in a gap it is necessary to reconstruct the injured nerve using an autograft or a graft from a compatible donor^[1,3]. One of the disadvantages of grafting is the necessity of a second surgery for collecting the nerve sample and respective donor site morbidity. In addition, non-matching donor and recipient nerve diameters often occur, which might be the reason for an incomplete functional recovery^[4]. Entubulation offers advantages compared to graft implantation, including the potential to manipulate and to improve the regeneration environment within the tube-guide by adding to the lumen, growth factors and/or cellular systems^[5]. Consequently, guidance of regenerating axons is improved by a mechanical effect but also by cellular growth factors, a chemical^[6] and electrical cues^[7]. Natural and synthetic biomaterials have been used as tube-guides, being the later sub-divided into two major groups: biodegradable and non-biodegradable^[8,9]. The development of tube-guides is a consequence of the limitations inherent in the use of grafts, in terms of length, diameter and type of fiber, preventing damage to the sampling local, as it was previously referred^[10]. For a correct nerve regeneration some important physical properties of tube-guides have been listed and referred by several authors like: the tube-guides should be made of biodegradable biomaterials with appropriate porous dimensions; the ability to deliver growth factors and drugs and allow the incorporation of cellular systems; an internal geometry to support an organized cell migration or intraluminal structures similar to nerve fascicles; and with some electrical activity in order to promote axon regeneration^[11]. The use of electric conductive biomaterials to achieve nerve regeneration is a promising research area^[12]. The goal of this work was to evaluate the therapeutic effect (by morphological and functional analysis) of three previously developed tube-guides with electrical conductivity for nerve regeneration associated to mesenchymal stem cells (MSCs) isolated from the Wharton's jelly of umbilical cord (UC) on neuro-muscular regeneration after neurotmesis injury using the rat sciatic nerve model. The three tube-guides used *in vivo* where those made of polyvinyl alcohol (PVA), PVA loaded with MWCNTs [functionalized carbon nanotubes (CNTs), PVA-CNTs], and PVA loaded with polypyrrole (PVA-PPy). Such composites with electric conductivity can be used to

host cell therapies, and beneficial regenerative electrical stimulation can be applied directly to the cells through the composite^[13]. PVA is a polymer used as a biomaterial due to its biocompatibility, non-toxic, non-carcinogenic, swelling properties, and bio-adhesive characteristics. PVA can also be used as host material in order to increase the solubility as well as the mechanical strength of conductive materials, and it is approved by Food and Drug Administration^[14,15]. PPy and CNTs are two of the most studied conductive polymers for tissue engineering, especially for nerve tissue engineering^[16]. The authors previously to *in vivo* application, focused on tube-guides design and *in vitro* characterization. The PVA-CNTs and PVA-PPy tube-guides presented conductivity advantages, important for nerve regeneration. The developed electrical conductive nerve tube-guides was achieved by loading PVA with 0.05% of PPy or COOH-functionalized CNTs. The inclusion of CNTs and PPy brought a significant increase of electrical conductivity of the simple PVA tube-guide. The PVA-CNTs tube-guides showed the rougher topography. The DSC and X-ray diffraction (XRD) studies revealed that all materials have similar low crystallinity. The wettability studies indicated a hydrophilic behaviour of all nerve tube-guides, being the PVA-PPy slightly more hydrophobic. In terms of surface charge, the zeta potential measurements revealed that both COOH-functionalized CNTs and PPy loads turned the surface charge slightly more positive. Regarding the elastic behaviour, the COOH-functionalized CNTs load caused a slight decrease of the rigidity of PVA. PVA-CNTs and PVA-PPy might present a regenerative potential and were tested in the rat sciatic nerve neurotmesis injury model^[17]. Also, since the PVA-CNTs presented the rougher topography, which is important for the association and viability of the associated cellular systems^[9], where also tested associated to the MSCs-based therapy^[3,18].

Considering the peripheral nerve system (PNS), MSCs are promising cell-based therapies to be applied alone or associated to scaffolds. MSCs have a high plasticity, proliferative and differentiation capacity, and also have the advantage of presenting immunosuppressive properties^[3,19,20]. For these reasons, MSCs have been used in experimental trials as cell-based therapies, including pathologies of PNS and central nervous system (CNS). Furthermore, nowadays the characterization of MSCs is well defined by recommendations and standards stated by the international society for cellular therapy (ISCT)^[19]. The MSCs therapeutic effect resides on their capacity to replace original cells of damaged tissues, and also by the physiologic secretion of growth factors and cytokines that modify the microenvironment inducing the activity of endogenous progenitor cells within the injured tissue, and by modulating the inflammatory and immune responses. The inflammatory modulation includes the Wallerian degeneration, a crucial step for nerve regeneration after neurotmesis injury^[3]. Therefore, the use of cellular systems is a rational approach for promoting nerve



Figure 1 Synthetic biodegradable tubes of polyvinyl alcohol, polyvinyl alcohol loaded with COOH-functionalized multiwall carbon nanotubes MWCNTs (polyvinyl alcohol-carbon nanotubes, polyvinyl alcohol-carbon nanotubes tube-guides), and polyvinyl alcohol loaded with polypyrrole (polyvinyl alcohol-polypyrrole, polyvinyl alcohol-polypyrrole tube-guides).

regeneration by delivering growth-promoting factors and cytokines at the nerve lesion site^[9]. MSCs can be isolated from several tissues, including bone marrow (BM), umbilical cord blood (UCB) and umbilical cord tissue (UCT), dental pulp, and adipose tissue^[9]. BM collection has several disadvantages, since the BM include a high percentage of adipocytes and a heterogeneous cell population, there is the possibility of morbidity associated to donor collection, as well as it is observed a decreasing number of BM-MSCs along the adult life and available for therapeutic applications. The research concerning other sources of MSCs has been intensively performed for the past years for identifying tissues that will allow MSCs isolation, and safe and controlled *ex vivo* expansion of these cells for potential allogeneic and autologous application^[9]. MSCs isolated from the Wharton's jelly UCT have been tested for the clinical application in CNS and PNS, including neurodegenerative diseases^[21]. It has been reported that MSCs from the UCT are still viable 4 mo after transplantation and there is no need for immunological suppression of the patients and experimental animals^[22]. The reason for this advantage is the fact that these cells are negative for major histocompatibility complex (MHC), and have low expression of MHC class I^[19] with potential application for MSC-based therapies in allogeneic treatments. *In vivo* studies involving these MSCs are limited but encouraging, especially what concerns PNS. Also, there are an increasing number of high quality cryopreserved cord tissue units in Cord Blood Banks worldwide. In addition, these cells represent a non-controversial source of MSCs, without neither ethical nor religious issues that are routinely harvested after birth, cryogenically stored, thawed, and can be expanded for therapeutic uses^[9]. On the other hand, it was demonstrated in some studies, that grafted MSCs have a signalling role which initiates the recruitment and direction of endogenous cells by growth factors production, promoting the local regeneration and modulating the inflammatory process^[23]. Nowadays it is believed that factors secreted

by MSCs are primarily responsible for their therapeutic action, so it is particularly important to understand and fully characterize the MSCs secretome^[18,24,25]. Recent studies demonstrated that MSCs produce and secrete multiple paracrine factors like interleukine-2 (IL-2), IL-6, IL-8, IL-12, IL-15, monocyte chemoattractant protein-1, macrophage inflammatory protein-1 β , regulated on activation, normal T cell expressed and secreted, and platelet-derived growth factor-AA. The several secreted factors previously listed that are present in MSCs conditioned medium (CM) was already described by others^[26] and more recently, by our research group^[18]. These paracrine factors are important to promote the MSCs therapeutic effects identified by the scientific community, like immunomodulatory and chemoattractive, anti-apoptotic, anti-fibrotic, angiogenic, and anti-oxidants activities. The hypothesis that MSCs and the growth factors produced during expansion in culture (CM) is an appropriate therapeutic product for local application in severe peripheral lesions seemed to be a rational approach and was studied in the present experimental work.

MATERIALS AND METHODS

Tube-guide preparation

Synthetic biodegradable tubes of PVA (Aldrich, Mowiol 10-98), PVA loaded with COOH-functionalized multiwall carbon nanotubes MWCNTs (Nanothinx, NTX5, MWCNTs 97% - COOH) (PVA-CNTs tube-guides), and PVA loaded with PPy (Aldrich, 10-40 S/cm of conductivity) (PVA-PPy tube-guides) were prepared using a casting technique to a silicone mould. A 15% (%w/v) aqueous solution of PVA was prepared. Then the solution of PVA was mixed with 0.05% of COOH-functionalized MWCNTs and 0.05% of PPy. The tube-guides were produced by freezing/thawing process. The treatment consisted in three cycles of freezer (-30 °C)/ incubator (25 °C), and an annealing treatment started with a stage of 14 h on an incubator (25 °C) followed by a ramp rate of 0.1 °C/min until 80 °C, and then a stage of 20 h at 80 °C. The tube-guides were sterilized by gama-radiation and hydrated in a sterile saline solution during 2 h before microsurgical application in the rat neurotmesis injuries (Figure 1).

MSCs cell culture and *in vitro* characterization

MSCs culture and expansion: Human MSCs isolated from the Wharton jelly (WJ) of UCT from PromoCell GmbH (C-12971, lot-number: 8082606.7) were cultured and expanded in a humidified atmosphere with 5% CO₂ at 37 °C by replacing the mesenchymal stem cell medium, PromoCell (C-28010) every 48 h. At 80% confluence, normally obtained after 4 d in culture (Figure 2), MSCs were harvested with 0.25% trypsin with EDTA (GIBCO) for further expansion at an initial concentration of 1 × 10⁴ cells/cm². Immediately previously to *in vivo* application, a MSCs suspension was prepared in 1 mL syringes. Each syringe contained MSCs at a concentration

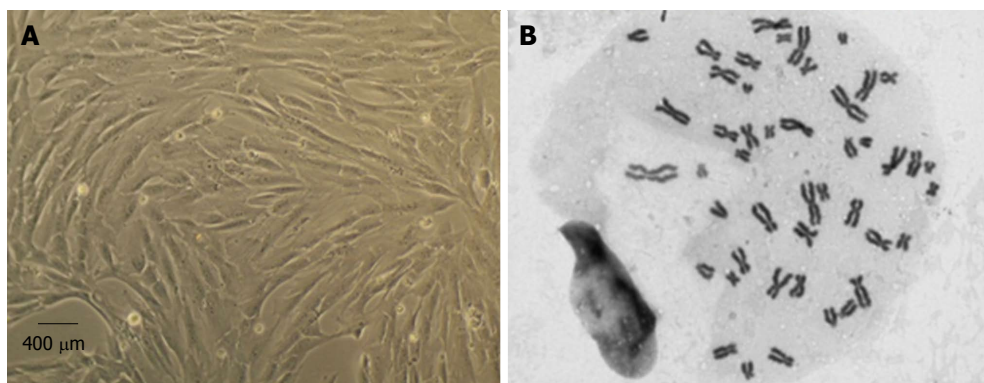


Figure 2 Mesenchymal stem cells culture and expansion. A: Isolated mesenchymal stem cells (MSCs) from the Wharton's jelly of umbilical cord presented a fusiform, fibroblast-like morphology in culture (magnification: 100 ×); B: Selected metaphases from MSCs in culture, showing normal number of chromosomes (46, XY) (magnification: 1000 ×).

of $1 \times 10^6/\mu\text{L}$ for posterior intra-operatively nerve injection.

The MSCs lot used in the present experimental study was characterized by flow cytometry analysis for a comprehensive panel of markers by PromoCell as previously reported^[18,25]. The MSCs exhibited a mesenchymal-like shape with a flat and polygonal morphology during cell culture expansion. Their phenotype was evaluated by flow cytometry for PE anti-human cluster of differentiation-105 (CD105); APC anti-human CD73; PE anti-human CD90; PerCP/Cy5.5 anti-human CD45; FITC anti-human CD34; PerCP/Cy5.5 anti-human CD14; Pacific Blue anti-human CD19 and pacific-blue anti-human Human Leukocyte Antigen-DR (HLA-DR) (antibodies and their respective isotypes from BioLegend).

MSCs karyotype by cytogenetic analysis: Cytogenetic analysis was carried out before *in vivo* application between passages 4 and 5 as previously reported^[18,25]. Chromosome analysis was performed by one scorer on 20 Giemsa-stained metaphases and each MSC cell was scored for chromosome number. For determination of the karyotype, a routine chromosome G-banding analysis was also carried out and no structural alterations were observed which demonstrates the chromosomal stability to the cell culture procedures and also that the *in vivo* applied MSCs are not neoplastic (Figure 2).

Cytocompatibility evaluation of biomaterials: Intracellular free Ca^{2+} concentration ($[\text{Ca}^{2+}]_i$) by using dual wavelength spectrofluorometry as previously described^[27] was measured in Fura-2-loaded MSCs cells. $[\text{Ca}^{2+}]_i$ from MSCs cultured without the presence of any biomaterial, sub-cultured over PVA discs, over PVA loaded with CNTs (PVA-CNTs) and PVA loaded with PPy (PVA-PPy) discs of 10 mm diameter are results obtained from epifluorescence technique confirming that the MSCs did not begin the apoptosis process.

Reverse transcriptase polymerase chain reaction to confirm that MSCs are undifferentiated: Reverse

transcriptase polymerase chain reaction (RT-PCR) and quantitative PCR (qPCR) targeting specific genes expressed by the MSCs that were *in vivo* applied was performed to certify that the MSCs used *in vivo* were not differentiated. For that, primers were designed targeting seven human genes based on the literature^[18]. DNA sequences from growth associated protein-43 (GAP-43), neurofilament-H (NF-H), Nestin, Glyceraldehyde-3-Phosphate Dehydrogenase (GAPDH), β -actin, neuronal nuclear (*NeuN*) and glial fibrillary acidic protein (*GFAP*) genes from mice (*Mus musculus*), rat (*Rattus norvegicus*) and human (*Homo sapiens*) were downloaded from GenBank (www.ncbi.nlm.nih.gov/genbank) and aligned using the Clustal Omega bioinformatic tool from EMBL-EBI (<http://www.ebi.ac.uk/Tools/msa/clustalo>). MSCs culture was harvested with 0.25% trypsin EDTA solution (Gibco) and centrifuged at 2000 rpm 4 °C during 5 min. Cell pellets were used for total RNA extraction using an adequate extraction kit, high pure RNA Isolation kit (Roche). Briefly, cell pellets were lysed with a lysis buffer, loaded into a High Pure Filter Tube, DNA was removed with DNase I enzyme, washed twice on column, and eluted with 100 μL of Elution Buffer. RNA was quantified and its quality assessed by using a Nanodrop ND-1000 Spectrophotometer and reads from 220 nm to 350 nm, and then stored at -80 °C until further use. In the following step, cDNA was synthesized from the purified RNA. To fulfill that issue, the kit Ready-To-Go You-Prime First-Strand Beads (GE Healthcare) was used following the manufacturer instructions. Briefly, 1.5 μg of total RNA was used and diluted in DEPC-treated water to a 30 μL final volume in a RNase-free microcentrifuge tube; then heated at 65 °C for 10 min and then chilled in ice; transfer the RNA solution to the kit tube containing the first-strand reaction mix beads; add 0.2 μg of Oligo(dT) primer and DEPC-treated water to a 33 μL final volume; mix the content and incubate at 37 °C for 60 min. cDNA was synthesized and stored at -20 °C until further use. Of referring that, due to the use of the Oligo(dT) primer, the synthesized cDNA corresponds to the mRNA present in the sample at the time of collection. cDNA synthesized from undifferentiated MSCs was used to

check the expression of seven genes, two housekeeping genes (β -actin and *GAPDH*) and five specific of neuronal cells (GFAP, NeuN, Nestin, NF-H and GAP-43). Primers were designed in house and then synthesized in an external laboratory (MWG Operon, Germany). The primers were rehydrated in DNase/RNase free water in a concentration of 100 pmol/ μ L. qPCR was performed in a iCycler[®] iQ5TM (BioRad) apparatus using the iQTM SYBR[®] Green Supermix (BioRad). Each pair of primers targeting a gene was used to analyze its expression in the MSCs cDNA, in triplicate, along with a negative control. The plates containing the mix targeting the seven genes for both types of cells were submitted to the following cycles of temperatures: 95 °C during 4 min, 35 cycles comprising 95 °C during 20 s, 55 °C during 20 s and 72 °C during 20 s ending with Real-Time acquisition, and final extension of 75 °C for 7 min. After cycling temperatures, the number of cycle threshold for each well was recorded. The plate containing the amplified genes or qPCR products was kept in ice and observed in a 2% agarose gel to check and reinforce the identity of the amplicons. Briefly, 2 g of NuSieve[®] 3:1 Agarose (Lonza) were mixed with 100 mL Tris-Acetate-EDTA buffer, melted, mixed with ethidium bromide in a final concentration of 0.2 μ g/mL, and loaded in a horizontal electrophoresis apparatus. After solidification, 15 μ L of the qPCR products were loaded in the agarose wells, and submitted to a 120 V potential difference during 40 min to separate the amplicons. Gel was then observed under UV light and pictures recorded using the GelDoc[®] 2000 (BioRad) and Quantity One[®] software (BioRad). In the MSCs, the molecular analysis showed a very small amplification of *GFAP* gene, absence of amplification of the *NF-H* and *GAP-43* genes, and reasonable amplification of *NeuN*, β -actin, *GAPDH* and *Nestin* genes. Amplification of a given gene is correlated with its expression seeing that the template DNA is the one generated from mRNA. The RT-PCR results confirmed that the MSCs used *in vivo* were not differentiated into neuro-glial cells.

Surgical procedure for the rat sciatic nerve model for neurotmesis

The article describes a basic research study involving animal subjects and was approved by the Veterinary Authorities of Portugal [Direcção Geral de Alimentação e Veterinária (DGAV)] in accordance with the European Communities Council Directive of November 1986 (86/609/EEC), and the National Institutes of Health (NIH) guidelines for the care and use of laboratory animals have been observed. Also all the authors involved in the *in vivo* tasks have a degree in Veterinary Medicine and are accredited by the Veterinary Authorities of Portugal (DGAV) and by Felasa - Category C for working with laboratory animals.

The OECD Guidance Document on the Recognition, Assessment and Use of Clinical Signs as Humane Endpoints for Experimental Animals Used in Safety Evaluation (2000) were always followed by the authors

by taking adequate measures to minimize pain and discomfort.

Polycarbonate cages type 3 were used for housing under standard laboratory conditions adult male Sasco Sprague Dawley rats with 300 g (Charles River Laboratories, Barcelona, Spain) always in a temperature and humidity controlled room with 12-12 h light/dark cycles. The rats were fed with standard chow and water *ad libitum* until the day of surgery. For surgery, the rats were anesthetized with ketamine 9 mg/100 g and xylazine 1.25 mg/100 g (body weight), by intraperitoneal administration. In lateral recumbence, the right sciatic nerve was exposed unilaterally and a transection injury was performed above the terminal nerve ramification using a straight microsurgical scissors, for creating a neurotmesis injury with 10 mm gap. Six experimental groups were studied: in groups 1, 2 and 3 after neurotmesis the proximal and distal nerve stumps were inserted 3 mm into PVA (group 1: PVA), PVA loaded with 0.05% (%w/v) of COOH-functionalized MWCNTs (group 2: PVA-CNTs), and PVA loaded with PPy 0.05% (%w/v) tube-guides (group 3: PVA-PPY), respectively, and tube-guides were sutured with two epineural sutures using 7/0 polypropylene monofilament, maintaining a nerve gap of 10 mm; in group 4 after neurotmesis, an autologous 180° inverted graft was sutured between both nerve stumps (group 4: Graft); in group 5 after neurotmesis, immediate cooptation with 7/0 monofilament polypropylene suture (group 5: End-to-End); in group 6 after neurotmesis the proximal and distal nerve stumps were inserted 3 mm in a PVA loaded with 0.05% (%w/v) of COOH-functionalized MWCNTs tube-guide kept in place with 2 epineural sutures using 7/0 monofilament polypropylene suture and the interior of the tube-guide was filled with 100 μ m of MSCs at a concentration of 1×10^5 cells/ μ L in culture medium, also 100 μ m of MSCs at a concentration of 1×10^6 cells/ μ L in culture medium were infiltrated in both nerve stumps inserted in the tube-guide (group 6: PVA-CNTs-MSCs) (Figure 3).

Functional assessment

After injury and sciatic nerve microsurgery reconstruction using the developed scaffolds in standardized neurotmesis injuries, a follow-up consisting in functional parameters measurements are important to evaluate the regeneration process and recovery. The animals were tested in an appropriate environment to minimize stress and handled by a single operator already trained for that purpose. Animals have been tested before the surgery at week 0, and after the surgery, at week 1, at week 2 and then every two weeks until the end of follow-up time of 20 wk.

Evaluation of motor performance and nociceptive function:

Motor performance was evaluated by measuring extensor postural thrust (EPT) and nociceptive function using the withdrawal reflex latency (WRL). The EPT included in the neurological recovery evaluation

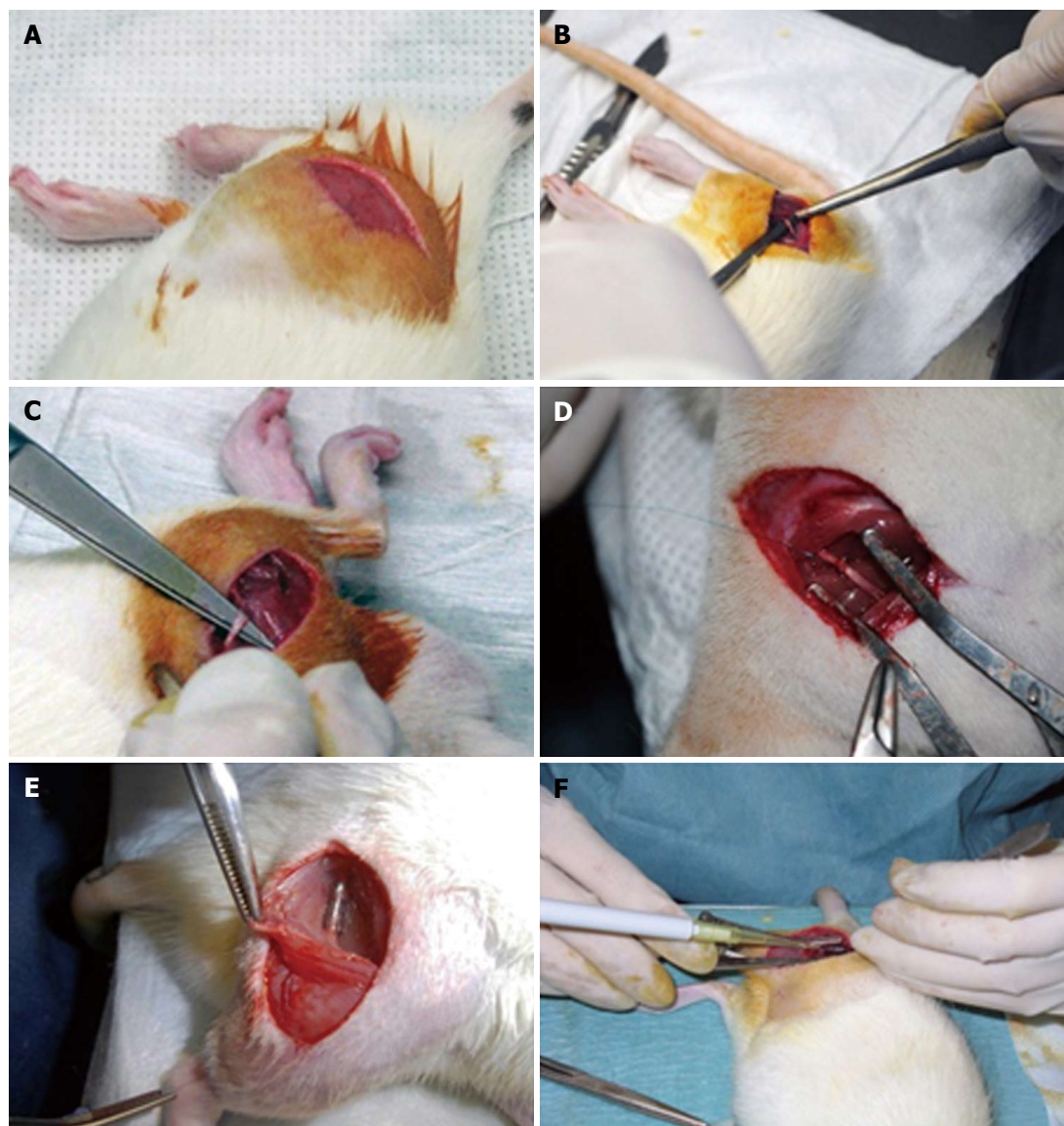


Figure 3 Surgery of the rat sciatic nerve neurotmesis injury model. Under deep anesthesia the right sciatic nerve was exposed unilaterally through a skin incision extending from the greater trochanter to the mid-half distally followed by a muscle splitting incision (A). After nerve mobilization (B), a transection injury was performed (neurotmesis) using a straight microsurgical scissors (C). In group 5 (End-to-End) after neurotmesis, immediate coaptation with 7/0 monofilament polypropylene suture was performed (D). Implantation of the tube-guide in the 10 mm gap (E). Local application of the mesenchymal stem cells (MSCs), the MSCs suspension filled the polyvinyl alcohol (PVA)-carbon nanotubes (CNTs) tube-guide lumen (group 6: PVA-CNTs-MSCs) (F).

of the rat after sciatic nerve injury was first described by^[28]. EPT is induced by lowering the affected hind-limb towards the platform of a digital balance supporting the animal by the thorax. During the test, the rat extends the hind-limb and the distal metatarsus and digits contact with digital platform balance. The force in grams (g) applied is recorded individually and the results for both hind-limbs (affected and un-affected hind-limb) are taken for equation 1 calculation. The normal (unaffected limb) EPT (NEPT) and experimental EPT (EEPT) values considered for equation (1) and the percentage of functional deficit is calculated^[9,28-31].

$$\% \text{ Motor deficit} = \left[\frac{\text{NEPT} - \text{EEPT}}{\text{NEPT}} \right] \times 100 \quad (1)$$

To assess the nociceptive WRL, the hotplate test

described by Masters *et al*^[32] was used with some modifications and previously described by the authors^[3,9,17,25,31,33]. Also, it is considered by the scientific bibliography that rats without sciatic nerve injury withdraw their paws from the hotplate within 4.3 s or less^[9,17,31,33]. If there was no paw withdrawal after 12 s, the animal was assigned the maximal WRL of 12 s and the heat stimulus was removed to prevent tissue damage^[34-36].

For sciatic functional index (SFI), a confined walkway measuring 42 cm long and 8.2 cm wide with a dark shelter at the end (own fabrication) that the rats cross was used. The footprints from the experimental (E) and normal (N) sides are measured: (1) distance from the heel to the third toe, the print length; (2) distance from the first to the fifth toe, the toe spread (TS); and (3) distance from the second to the fourth toe,

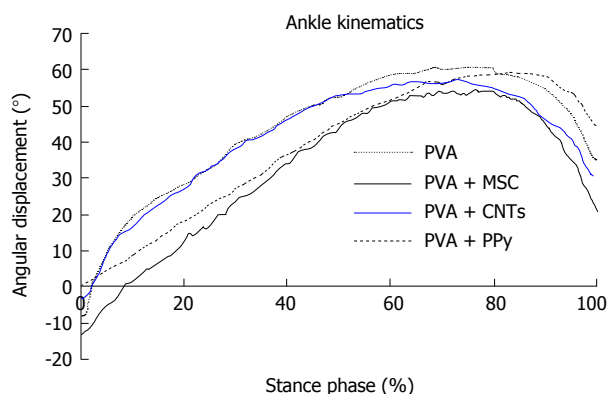


Figure 4 Kinematic plots in the sagittal plane for the ankle angle (°) as it moves through the stance phase, during the transection injury study. The mean of each group is plotted. PVA: Polyvinyl alcohol; CNTs: Carbon nanotubes; PPy: Polypyrrole; MSCs: Mesenchymal stem cells.

the intermediary toe spread (ITS). In the static sciatic functional index (SSI) is a simpler test where only the parameters TS and ITS are the measurements included in equation (6). Prints for measurements are chosen at the time of walking based on precise, clear and completeness of footprints^[9,36,37]. The mean distances of 3 measurements are used to calculate the following factors (dynamic and static):

$$TSF = (ETS - NTS)/NTS \quad (2)$$

$$ITSF = (EITS - NITS)/NITS \quad (3)$$

$$PLF = (EPL - NPL)/NPL \quad (4)$$

TSF: Toe spread factor; ITSF: Intermediate toe spread factor; PLF: Print length factor; ETS: Experimental toe spread; NTS: Normal toe spread; NITS: Normal intermediary toe spread; EITS: Experimental Intermediary toe spread; NPL: Normal print length; EPL: Experimental print length.

SFI is calculated as described by Bain *et al.*^[38] according to the following equation:

$$SFI = -38.3 \times (EPL - NPL)/NPL + 109.5 \times (ETS - NTS)/NTS + 13.3 \times (EITS - NITS)/NITS - 8.8 = (-38.3 \times PLF) + (109.5 \times TSF) + (13.3 \times ITSF) - 8.8 \quad (5)$$

Considering the SFI measurements, it was not possible to obtain values during the 20 wk follow-up after the surgery procedure, due to autotomy of the fingers. As a matter of fact, the rat sciatic nerve model for neurotmesis has this disadvantage; the autotomy observed in several experimental animals even when a repellent substance is applied routinely^[9]. SSI was calculated as described by^[39] according to the following equation (equation 6):

$$SSI = 108.4 \times TSF + 31.85 \times ITF - 5.49 \quad (6)$$

For SFI and SSI, when no footprints are measurable,

the index score of -100 is given considering total impairment, on the other hand, a score of 0 means that there is no alteration and the footprint is normal.

Kinematic analysis: Ankle kinematics was carried out at the end of the 20-wk follow-up time in the following experimental groups: PVA, PVA-CNTs, PVA-PPy, Graft, End-to-End, and PVA-CNTs-MSCs. A Perspex track with length, width (adjustable) and height of 120, 12, and 15 cm, respectively was used to record the rat locomotion in a straight line. The animals' gait was video recorded at a rate of 300 Hz images per second (Casio Exilim PRO EX-F1, Japan) by a camera with a visualization field of 14 cm wide, that was positioned at the track half-length, and 1 m distant from the track, where gait velocity was steady. The software APAS® (Ariel Performance Analysis System, Ariel Dynamics, San Diego, United States) was used for data analysis. The authors used a two-segment model of the ankle joint, adopted from the model firstly developed by^[40] (2D biomechanical analyses in sagittal plan), and the rat ankle angle was determined using the scalar product between a vector representing the foot and a vector representing the lower leg. Dorsiflexion and plantarflexion is considered for positive and negative values of position of the ankle joint (θ°). Initial contact (IC), opposite toe off (OT), and heel rise (HR) and toe-off (TO)^[33,40] were the time points analyzed for each step cycle, the values were time normalized for 100% of step cycle. The normalized temporal parameters were averaged over all recorded trials (Figure 4). Since the animal's normal walking velocity is 20-60 cm/sa^[33,40], stance phases lasting between 150 and 400 ms were considered for analysis.

Morphological analysis and histopathology: For histomorphometric analysis, nerve samples obtained from the 10-mm-long sciatic nerve segments distal to the neurotmesis site and from un-operated controls^[41-44]. The histological nerve preparation followed the previously reported protocol^[3,9,17,25,31,33,35] and a systematic random sampling and D-disector were adopted^[41-44].

At the end of the healing period tested (week 20), tibialis anterior (TA) muscles of all experimental (PVA, PVA-CNTs, PVA-PPy, Graft, End-to-End, and PVA-CNTs-MSCs) and Control (no lesion) groups were collected, and the tissue samples were fixed in 10% buffered formalin, routinely processed, dehydrated and embedded in paraffin wax. Consecutive 3 μ m transverse sections from the mid-belly of each muscle were cut, stained with haematoxylin and eosin (HE) and used for morphometry evaluation and determination of the degree of atrophy. For the morphometric analysis, an unbiased sampling procedure was applied and the following measures were calculated: area, perimeter, "Feret's angle" and "minimal Feret's diameter" (which is the minimum distance of parallel tangents at opposing borders of the muscle fiber). These parameters were evaluated from the cross sections using the ImageJ® software (NIH) which allowed to apply this set of individual fiber measurements. A

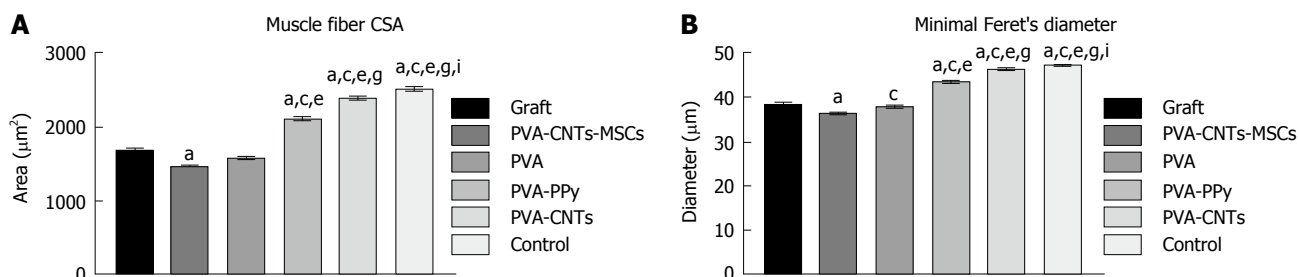


Figure 5 Graphical representation of the mean of area (A) and "minimal Feret's diameter" (B) of control, regenerated tibialis anterior muscle fibers at week-20 after neurotmesis (Graft) and neurotmesis with the proximal and distal nerve stumps sutured to a polyvinyl alcohol (polyvinyl alcohol) tube and polyvinyl alcohol coated tubes (polyvinyl alcohol, polyvinyl alcohol polypyrrole and polyvinyl alcohol carbon nanotubes). Values are presented as mean \pm SEM. ^a $P < 0.05$ vs Graft; ^c $P < 0.05$ vs Graft PVA CNTs MSCs; ^e $P < 0.05$ vs Graft PVA; ^g $P < 0.05$ vs Graft PVA PPy; ⁱ $P < 0.05$ vs Graft PVA CNTs. PVA: Polyvinyl alcohol; CNTs: Carbon nanotubes; PPy: Polypyrrole; MSCs: Mesenchymal stem cells.

minimum of 1000 skeletal muscle fibers was measured from each group. This assessment was performed by 2 independent operators. Each one of the operators measured, blindly and randomly, an average of 50 fibers in each section. Images were acquired using a Nikon[®] microscope connected to a Nikon[®] digital camera DXM1200, at low magnification (100 \times) under the same conditions that were used to acquire a reference ruler.

At the end of the study, all animals were subjected to a complete necropsy examination in order to evaluate the presence of possible internal anomalies and/or injuries. Lung, heart, kidneys, liver and spleen were collected and weighed and then submitted to histological analysis to check whether there were related microscopic changes such as inflammation, degeneration, or accumulation of biological material. The organs were fixed in 10% buffered formalin and processed for routine histology with HE stain. Microscopically, massive carbon deposits generally appear as well-recognized anthracotic black pigment, especially in the lung. A recent report described that some types of carbon nanotubes may appear as small punctuated accumulations inside Kupfer cells (liver) and in the intermediate zone of the spleen, when intravenously administered^[45]. Special stains, such as Von Kossa (method that demonstrates phosphates and carbonates) and Masson-Fontana (method used for distinguish carbon deposits from melanin) were also performed in consecutive sections.

Statistical analysis

The statistical review of the study was performed by a biomedical statistician [PAS Armada-da-Silva, CIPER-Faculdade de Motricidade Humana (FMH): Centro Interdisciplinar de Estudo de Performance Humana, FMH, Universidade de Lisboa, Estrada da Costa, 1499-002, Cruz Quebrada - Dafundo, Portugal].

A mixed model repeated measures ANOVA was used to test for differences across time and sciatic nerve treatment. Sphericity was assessed by Mauchly's test and Greenhouse-Geisser degrees of freedom correction was used in cases sphericity could not be assumed or when corrected P -values were below the accepted level of significance ($P < 0.05$). Tukey's HSD test was used for pairwise comparisons. All data is presented as mean

and standard deviation, unless otherwise stated. These statistical tests were carried out with IBM SPSS Statistics version 19. For stereology, statistical comparisons of quantitative data were subjected to one-way ANOVA test, followed by pairwise comparisons using Tukey's HSD test. Statistical significance was established as $P < 0.05$. Stereological data was analyzed using the software using the SPSS version 19.0 (SPSS, Chicago, IL). For muscle morphometry, statistical analysis was performed using the SPSS version 19.0 (SPSS, Chicago, IL). Results are presented as mean \pm scanning electron microscope (SEM) in Figures 5 and 6. Multiple comparisons between groups were performed by one-way ANOVA supplemented with Tukey's HSD post hoc test. Differences were considered statistically significant at $P < 0.05$.

RESULTS

Development and characterization of MSCs isolated from UC WJ

MSCs are defined by the ISCT which includes the following characteristics: (1) their capacity to adhere to plastic surfaces during cell culture; (2) expression of the specific surface markers (positive for CD73, CD90, and CD105, and no expression of CD14, CD19, CD34, CD45 and HLA-DR); and (3) are able to undergo tri-lineage differentiation into adipocytes, chondrocytes and osteoblasts^[19]. MSCs isolated from the UCT were expanded to P5-P6 where the culture appeared homogeneous and cells presented their typical fusiform, fibroblast-like, morphology (Figure 1). Flow cytometry analysis performed previously to *in vivo* application to expanded MSCs showed that over 95% of the cells in the population were consistently positive for the cell surface markers CD44, CD73, CD90 and CD105 and less than 2% positive for CD14, CD19, CD31, CD34, CD45 and HLA-DR. Also, the phenotype of MSCs was assessed by PromoCell by flow cytometry analysis for an additional comprehensive panel of markers: PECAM (CD31), HCAM (CD44), CD45, and Endoglin (CD105). Overall, these results are the ones expected for MSC-type stem cells according to ISCT^[19].

Giemsa-stained cells of MSCs at P5 were analyzed

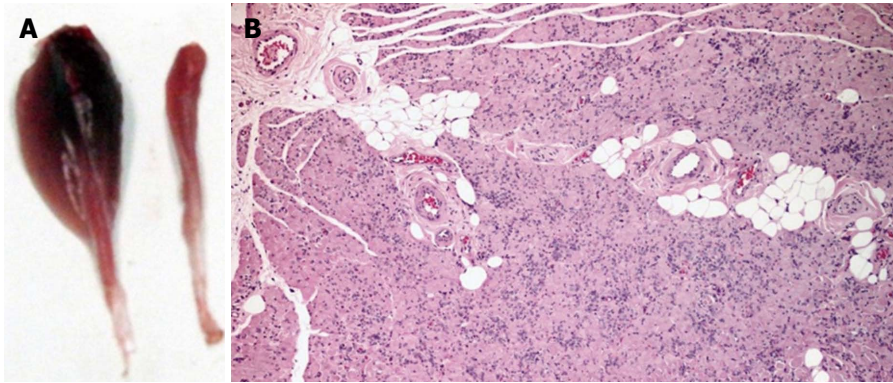


Figure 6 Macroscopic appearance of control tibialis anterior muscle and histological haematoxylin and eosin staining of a transverse section of tibialis anterior muscle. A: Macroscopic appearance of control tibialis anterior (TA) muscle (left) and 20 wk following neurotmesis and surgical treatment with PVA CNTs MSCs (right); B: Histological haematoxylin and eosin staining of a transverse section of TA muscle from PVA CNTs MSCs group. Magnification 40 ×. PVA: Polyvinyl alcohol; CNTs: Carbon nanotubes; MSCs: Mesenchymal stem cells.

for cytogenetic characterization. The karyotype of MSCs was determined previously to *in vivo* application to ensure that no neoplastic cells were used proving the cell therapy safety. The karyotype analysis demonstrated that no structural alterations were found, as well as chromosomal stability in terms of number and structure of the somatic and sexual chromosomes, to the cell culture procedures. The transplanted MSCs also presented normal morphology and flow cytometry markers for MSCs according to ISCT^[19].

Results obtained from epifluorescence technique confirmed that MSCs did not begin the apoptosis process, showing that the *in vivo* applied MSCs were viable even in the presence of the tube-guides biomaterials. The $[Ca^{2+}]_i$ measured was 47.9 ± 4.5 ($n = 25$), 46.2 ± 3.5 ($n = 25$) and 48.1 ± 3.9 ($n = 25$) for MSCs cultured in the presence of PVA, PVA-CNTs, and PVA-PPy discs after 7 d of culture, respectively. The MSCs cultured and expanded in the presence of the three tested biomaterials reached confluence and exhibited a normal star-like shape with a flat morphology in culture. According to these results, it is reasonable to conclude that the three biomaterials (PVA, PVA-CNTs, and PVA-PPy) are viable substrate for MSCs culture and survival and may be used in the pre-clinical trials.

The MSCs were harvested and its RNA purified and converted to cDNA using adequate procedures. Primers targeting markers, two housekeeping genes (β -actin and *GAPDH*) and five specific of neuronal cells (GFAP, NeuN, Nestin, NF-H and GAP-43) were used to support the fact that the MSCs used *in vivo* were not differentiated into neuro-glial cells. The molecular analysis showed a very small amplification of GFAP gene, absence of amplification of the NF-H and GAP-43 genes, and reasonable amplification of *NeuN*, β -actin, *GAPDH* and Nestin genes. Amplification of a given gene is correlated with its expression seeing that the template DNA is the one generated from mRNA. According to the results of RT-PCR, the molecular analysis showed a small expression of *GFAP* gene and absence of expression of the NF-H and *GAP-43* genes in the expanded MSCs.

Biomaterials characterization

The electrical conductivity achieved for the different tube-guides (PVA, PVA-CNTs and PVA-PPy) was the following: $1.5 \pm 0.5 \times 10^{-6}$ S/m, $579 \pm 0.6 \times 10^{-6}$ S/m, and $1837.5 \pm 0.7 \times 10^{-6}$ S/m, respectively. Therefore these three tube-guide [simple PVA, PVA loaded with 0.05% (%w/v) of COOH-functionalized CNTs and PPy] compositions were chosen for further characterization and for *in vivo* application in the rat sciatic nerve neurotmesis injury model. The thermal characteristics of simple PVA and loaded PVA materials was examined by differential scanning calorimetry and enthalpy of fusion (ΔH) was calculated, and the percentage of crystallinity was near 7.4% for all analyzed nerve guide tubes. Fourier transform infrared spectroscopy analysis the bands identified for PVA loaded with COOH-functionalized CNTs were similar of the bands detected for simple PVA. For PVA loaded with PPy new bands appeared at 1313/cm (C - N stretching vibration in the ring) and 1170/cm (C - H in-plane deformation). Compared with simple PVA the other nerve guide tubes showed a less intensity of the peaks, especially between 2237 and 2380/cm (unpublished data). Considering the XRD analysis previously performed, the broad peak observed at 20° corresponded to a typical diffraction peak of PVA, and it could be also observed in all tube-guides. Near 26° a broad scattering peak appeared for the tube loaded with PPy, and it was an indication of the presence of PPy as supported in literature^[46]; (unpublished data).

Both PVA and PVA loaded with PPy when analyzed by SEM exhibited similar surface appearance. On the other hand, the PVA loaded with COOH-functionalized CNTs showed a rougher surface as expected due to the presence of CNTs on PVA matrix, with oriented features. This characteristic was determinant to choose this biomaterial to be associated to the MSCs (PVA-CNTs-MSCs group). The Wettability analysis showed a hydrophilic behavior for the three biomaterials used for tube-guide tested, also the three materials showed negative zeta potential being the PVA the most negative

Table 1 Static sciatic functional index

SSI		Time											
		T0	T1	T2	T4	T6	T8	T10	T12	T14	T16	T18	T20
Group 1: PVA (n = 7)	Mean	-3.13	-40.52	-52.76	-69.60	-60.30	-56.59	-63.51	-54.89	-40.25	-44.03	-57.34	-48.23
	SD	24.17	19.25	17.78	9.56	19.69	13.19	8.05	11.96	13.33	9.07	21.81	7.25
Group 2: PVA-CNTs (n = 7)	Mean	12.10	-41.85	-45.81	-68.07	-51.18	-52.22	-49.31	-44.52	-48.73	-37.65	-38.47	-38.99
	SD	34.10	20.82	23.21	17.00	11.41	41.96	21.11	17.62	26.31	20.78	17.97	31.11
Group 3: PVA-PPy (n = 7)	Mean	5.31	-41.40	-50.95	-45.76	-47.40	-34.56	-39.51	-31.52	-32.47	-43.17	-50.00	-36.08 ^b
	SD	17.51	17.52	23.99	29.92	22.53	14.00	25.05	15.10	20.78	25.52	11.77	16.09
Group 4: Graft (n = 4)	Mean	-6.29	-56.46	-52.18	-55.41	-63.81	-59.79	-75.56	-53.15	-64.53	-67.22	-57.95	-52.07
	SD	1.59	28.10	27.54	27.99	19.06	11.00	10.45	15.44	12.14	12.17	8.31	9.76
Group 5: End-to-End (n = 5)	Mean	-5.78	-44.21	-33.72	-58.28	-73.92	-70.22	-52.47	-68.04	-41.91	-46.56	-43.04	-59.97
	SD	12.91	15.34	15.72	22.25	6.82	6.44	27.43	11.02	24.55	16.79	12.31	2.64
Group 6: PVA-CNTs-MSCs (n = 7)	Mean	3.46	-31.48	-23.75	-28.57	-39.97	-40.30	-62.32	-34.71	-26.28	-42.87	-37.54	-36.16 ^b
	SD	12.35	21.89	19.70	9.96	9.20	21.72	18.07	16.44	15.31	25.75	10.06	14.87

Static sciatic functional index (SSI) measured pre-operatively (week-0), and every week after the surgical procedure until week-20. An index score of 0 is considered normal and an index of 100 indicates total impairment. The measurements of the toe spread (TS), and the intermediary TS, were taken from the experimental (E) and normal (N) sides. Results are presented as mean and SD. *n* corresponds to the number of rats within the experimental group. PVA: Polyvinyl alcohol; CNTs: Carbon nanotubes; PPy: Polypyrrole; MSCs: Mesenchymal stem cells. ^b*P* < 0.01 vs Graft.

surface (-4.97 mV) (Figure 2).

Functional analysis during the healing period of 20 wk

SFI and SSI analysis: A few SSI data were missing due to inability to collect visible fingerprints as it was previously referred. As a result of the limited number of animals and the limitations of repeated measures analysis, missing SSI values were replaced using interpolation. Nine of a total of 275 SSI values were interpolated with only one animal having two missing values replace using the linear interpolation procedure. Also because of missing values, the 2-wk time point was not considered for statistical analysis. Sciatic nerve neurotmesis caused a steep decrease in SSI scores in every experimental group and therefore a significant effect of time could be found [$F(10, 200) = 20.445$; $P < 0.001$]. SSI scores remained negative and with little changes throughout the time following sciatic nerve neurotmesis and independently from sciatic nerve treatment, leading to a non-significant time vs treatment interaction effect [$F(40, 190) = 279.581$; $P < 0.651$]. However, there was significant differences in the extent of SSI scores' decrease between the experimental groups [$F(4, 20) = 5.848$; $P < 0.01$], with PVA-PPy tube-guides ($P < 0.01$) and PVA-CNTs-MSCs ($P < 0.01$) groups showing less severe SSI scores compared with Graft group (Table 1).

The motor performance by SFI was not possible to perform due to autotomy observed in all treated animals.

Evaluation of motor performance (EPT) and nociceptive function (WRL)

WRL: In the weeks following sciatic nerve neurotmesis there was a large increase in the time latency to withdraw the paw in response to the thermal stimulus, with most animals reaching the cut-off time of 12 s and leading to a significant effect of time [$F(11, 341) = 17.944$; $P < 0.001$]. A mild improvement in latency times occurred over the weeks of recovery

at a rate that was similar between the experimental groups so that no significant interaction effect existed [$F(55, 341) = 5.727$; $P < 0.503$]. According to ANOVA results, differences between treated groups (PVA, PVA-CNTs, PVA-PPy, PVA-CNTs-MSCs, Graft and End-to-End) in the severity of changes in WRL times existed [$F(5, 31) = 2.942$; $P < 0.05$], but these differences were not large enough to be detected by the pairwise comparisons (Table 2).

The motor performance by EPT was not possible to perform due to autotomy observed in all treated animals.

Ankle joint kinematics: Measures of ankle joint angle at the four selected instants of the stance phase (IC, OT, HR and TO) were collected at the end of 20-wk recovery period. This analysis was carried out only for biomaterial (PVA, PVA-CNTs and PVA-PPy groups, $n = 7$) and biomaterial plus MSCs-treated animals (PVA-CNTs-MSCs group, $n = 7$). Ankle joint angle values were similar across the experimental groups at the times of IC, OT and HR ($P =$ non-significant). However, at TO less acute ankle joint angles were seen for PVA-CNTs-MSCs group, compared with PVA-PPy group ($P < 0.01$) and with PVA-CNTs group showing similar trend also compared with PVA-PPy group ($P = 0.051$). Such less acute ankle joint angles might suggest improved ankle muscles function during the push off phase of the rat's gait cycle (Table 3 and Figure 4).

Morphological analysis

Muscle results: After the healing period of 20 wk, TA muscle of all treated rats from the experimental groups (PVA, PVA-CNTs, PVA-PPy, PVA-CNTs-MSCs, Graft and End-to-End) was collect for histological analysis and morphometry to evaluate the secondary neurogenic muscle atrophy associated to neurotmesis injury. It was also evaluated the muscle healing process that followed the sciatic nerve regeneration where the scaffold

Table 2 Withdrawal reflex latency

WRL		Time											
		T0	T1	T2	T4	T6	T8	T10	T12	T14	T16	T18	T20
Group 1: PVA (n = 7)	Mean	3.71	10.95	10.81	10.68	9.74	10.23	9.85	8.15	7.78	9.99	7.88	6.98 ^a
	SD	0.93	1.45	2.04	2.26	2.89	2.50	2.81	2.70	3.50	2.49	3.72	3.72
Group 2: PVA-CNTs (n = 7)	Mean	5.36	9.91	8.98	7.50	8.40	9.48	9.51	6.92	6.60	8.43	5.88	5.83 ^a
	SD	1.50	3.57	3.65	3.36	3.22	3.41	3.01	3.49	3.41	3.40	3.09	2.80
Group 3: PVA-PPy (n = 7)	Mean	4.86	11.42	9.37	7.10	7.85	8.82	9.72	6.87	7.02	7.09	6.06	7.02 ^a
	SD	1.69	1.54	3.31	2.51	3.40	2.53	2.35	3.50	3.92	3.23	4.43	3.89
Group 4: Graft (n = 4)	Mean	4.53	12.00	10.14	11.17	11.50	10.67	10.83	11.16	9.81	10.46	9.92	9.68 ^a
	SD	1.14	0.00	3.72	1.66	1.01	2.65	2.35	1.27	2.84	1.78	1.82	1.88
Group 5: End-to-End (n = 5)	Mean	4.28	12.00	11.85	12.00	10.22	10.45	8.78	10.48	9.26	8.57	9.82	7.50
	SD	0.86	0.00	0.34	0.00	2.50	2.12	2.22	2.86	3.07	0.98	2.02	0.87
Group 6: PVA-CNTs-MSCs (n = 7)	Mean	3.93	12.00	8.89	9.23	9.30	9.90	7.65	7.41	10.06	8.33	8.28	8.02 ^a
	SD	0.86	0.00	2.36	1.63	2.72	2.66	2.51	2.33	1.85	2.86	2.34	1.20

Values in seconds were obtained performing withdrawal reflex latency (WRL) test to evaluate the nociceptive function. This test has been performed pre-operatively (week-0), at week 1, week 2 and every 2 week after the surgical procedure until week-20, when the animals were sacrificed for morphological analysis. Results are presented as mean and standard error of the mean (SD). *n* corresponds to the number of animals within each experimental group. PVA: Polyvinyl alcohol; CNTs: Carbon nanotubes; PPy: Polypyrrole; MSCs: Mesenchymal stem cells. ^a*P* < 0.05 vs End-to-End.

Table 3 Ankle kinematics

Temporal events	Group	Week 20
IC	Group 1: PVA	-3.23 ± 20.65
	Group 2: PVA-CNTs	-8.32 ± 17.36
	Group 3: PVA + PPy	0.82 ± 26.33
	Group 6: PVA-MSCs	-13.68 ± 8.57
OT	Group 1: PVA	28.30 ± 19.52
	Group 2: PVA-CNTs	27.67 ± 12.91
	Group 3: PVA + PPy	17.66 ± 13.20
	Group 6: PVA-MSCs	11.43 ± 9.69
HR	Group 1: PVA	46.67 ± 14.81
	Group 2: PVA-CNTs	47.69 ± 11.19
	Group 3: PVA + PPy	36.46 ± 10.14
	Group 6: PVA-MSCs	34.07 ± 6.85
TO	Group 1: PVA	33.99 ± 9.57
	Group 2: PVA-CNTs	27.01 ± 10.99
	Group 3: PVA + PPy	43.90 ± 8.76
	Group 6: PVA-MSCs	20.56 ± 11.31

Values were obtained performing video analysis at 20-wk of the healing period. Results are presented as mean and standard deviation (SD) (*n* = 7). For each step cycle the following time points were identified: Initial contact (IC), opposite toe off (OT), heel rise (HR) and toe-off (TO). PVA: Polyvinyl alcohol; CNTs: Carbon nanotubes; PPy: Polypyrrole.

was applied. It was possible to observe by muscle morphometry that there was a significant difference (*P* < 0.05) in terms of the increase in mean fiber size between some of the treatment (PVA-PPy and PVA-CNTs) groups and the Graft group. In fact, in the PVA-PPy group there was a 25% increase in terms of average fiber area and a 13% increase in terms of the "minimal Feret's diameter", when compared to the Graft group. Whereas in the PVA-CNTs treatment group there was a 42% increase in terms of average fiber area and a 21% increase in term of the "minimal Feret's diameter", when compared to the Graft group. Although both these two treatment groups (PVA-PPy and PVA-CNTs) exhibited significant improvement in fiber size, approaching the values for normal muscles (collected from rats with no sciatic nerve neurotmesis lesion), both of them were

still significantly different (*P* < 0.05) from the control group (without lesion) at 20 wk after lesion. PVA treatment without any coating (PVA group) revealed no regeneration benefit since the mean fiber size was lower (with significant difference in terms of "minimal Feret's diameter"; *P* < 0.05) when compared to the Graft group (Figure 5). However, unexpected results were observed with PVA-CNTs-MSCs, which showed the worst results in terms of muscular atrophy after denervation, results not correlated with functional analysis (considering mostly kinematics gait analysis and SSI) (Figure 5). The decreased fiber size observed in these animals' TA muscles was coincident with the smaller sized muscles that were collected at 20 wk after surgery macroscopically evaluated during the collection for histological evaluation. Histologically it was also possible to detect a considerable amount of necrosis with delayed muscle regeneration in this group's muscles (Figure 6).

Histomorphometry of the regenerated sciatic nerve: Histological analysis showed that nerve fiber regeneration occurred in all reconstructed nerves. In comparison to controls (sciatic nerve without neurotmesis injuries, data not shown)^[3], in all repaired nerves regenerated fibers showed small axons with thin myelin sheaths and microfasciculation (Figure 7). Microfasciculation was more evident in the PVA-CNTs-MSCs repaired group (Figure 7 and Table 4). Also, stereological analysis disclosed a significantly (*P* < 0.05) larger axon diameter, but not fiber diameter, in the regenerated nerves from PVA-PPy group compared with those from PVA-CNT-MSC group (Table 4). On the other hand, as it was previously reported^[3,25], the application of MSCs-based cell therapy to neurotmesis nerve injuries resulted in a significantly increased myelin thickness (M), ratio myelin thickness/axon diameter (M/d) and ratio axon diameter/fiber diameter (d/D; g-ratio) when compared to PVA, PVA-CNTs, PVA-PPy groups (*P* < 0.05). The results clearly demonstrate a

Table 4 Stereological quantitative assessment

Group		Density	Total number	Axon diameter (d)	Fiber diameter (D)	Myelin thickness (M)	M/d	D/d	d/D (g-ratio)	Area (mm ²)
Group 1: PVA (n = 7)	Mean	42872	16596	2.95	3.56	0.31 ^a	0.11 ^a	1.23	0.82 ^a	0.3862
	SD	4007	1741	0.25	0.28	0.03	0.01	0.02	0.01	0.0772
Group 2: PVA-CNTs (n = 7)	Mean	36261	16049	2.98	3.71	0.37 ^a	0.14 ^a	1.28	0.79 ^a	0.4455
	SD	4267	1172	0.25	0.27	0.01	0.01	0.03	0.01	0.1856
Group 3: PVA-PPy (n = 7)	Mean	40289	22588	3.03 ^a	3.70	0.33 ^a	0.12 ^a	1.24	0.81 ^a	0.5720
	SD	2686	3157	0.21	0.23	0.02	0.01	0.01	0.00	0.2565
Group 4: Graft (n = 4)	Mean	37041	21939	2.58	3.56	0.49	0.21	1.41	0.71	0.5936
	SD	1214	1302	0.06	0.08	0.02	0.01	0.02	0.01	0.0694
Group 5: End-to-end (n = 5)	Mean	38762	22729	2.65	3.58	0.47	0.19	1.38	0.73	0.5990
	SD	1524	2308	0.14	0.16	0.01	0.01	0.01	0.01	0.2082
Group 6: PVA-CNTs-MSCs (n = 7)	Mean	43373	25731	2.44	3.34	0.45 ^{c,e}	0.21 ^{c,e}	1.41	0.72 ^{c,e}	0.5942
	SD	3881	3386	0.20	0.21	0.06	0.04	0.08	0.01	0.1940

Density, total number, axon diameter (d), fiber diameter (D), myelin thickness (M), ratio myelin thickness and axon diameter (M/d), ratio fiber diameter and axon diameter (D/d), ratio axon diameter and fiber diameter (d/D, g-ratio) of regenerated sciatic nerve fibers at week-20 after neurotmesis. Values are presented as mean ± SD. *n* corresponds to the number of animals within each experimental group. PVA: Polyvinyl alcohol; CNTs: Carbon nanotubes; PPy: Polypyrrole. ^a*P* < 0.05 vs PVA-CNT-MSC; ^c*P* > 0.05 vs End-to-End; ^e*P* > 0.05 vs Graft.

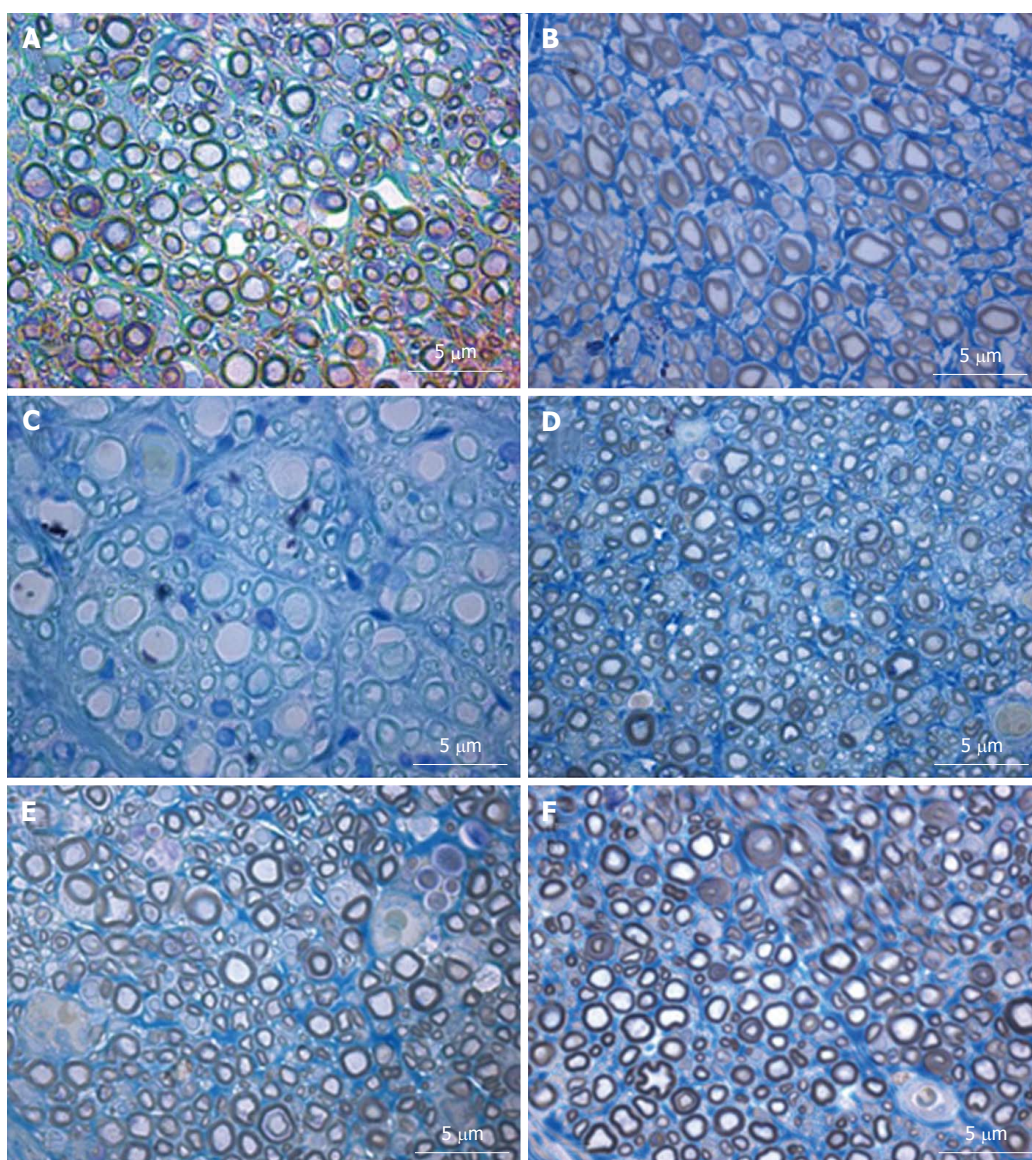


Figure 7 Histological appearance of regenerated nerve fiber in the different groups of neurotmesis. A: PVA; B: PVA-CNTs; C: PVA-PPy; D: PVA-CNTs-MSCs; E: Graft; F: End-to-end suture (magnification: 1000 x). PVA: Polyvinyl alcohol; CNTs: Carbon nanotubes; PPy: Polypyrrole; MSCs: Mesenchymal stem cells.

synergistic positive effect on regenerated nerve fibers resulting from combined use of MSCs with the PVA-CNTs tube-guides. Also, in the PVA-CNTs-MSCs group these three stereological parameters (M, M/d, and g-ratio) were not significantly different from the values obtained from End-to-End and Graft groups (Table 4). The total number of nerve fibers and nerve fibers density were similar in all groups.

Histology of internal organs: At the microscopic exam, no alterations were observed. The histology sections of all organs confirmed the absence of inflammation, cell degeneration, necrosis and fibrosis. No signs of nanotubes, neither carbon deposits were detected in all organs.

DISCUSSION

An organ re-innervation and functional recovery after nerve injury has been intensively studied worldwide and regenerative medicine methods including cellular systems and new biomaterials concerning the peripheral nerve have been developed. The involved mechanisms in the regeneration process and the ideal scaffold have not been discovered yet. Peripheral nerve might regenerate after some types of injury like axonotmesis but it is difficult to achieve functional recovery after neurotmesis, especially when there is loss of nerve tissue and a gap is created. In the peripheral nervous system, nerves after axonotmesis injuries can regenerate, without any treatment but in most clinical cases a muscle regional neurogenic atrophy occurs. When neurotmesis injuries occur, the nerves must be surgically treated by direct end-to-end suture^[33,47,48], using appropriate microsurgery techniques and suturing material. Nowadays most tissue engineered nerve grafts are composed of a neural scaffold prepared with a variety of biomaterials, and surgically applied in neurotmesis injuries with loss of nervous tissue where the direct end-to-end suture is not possible creating tension in the suture line and compromising the nerve regeneration^[9]. The introduction of cell therapies should be delivered by appropriate vehicles promoting an important biochemical and physical cue. MSCs represent an appealing source of adult stem cells for cell therapy and tissue engineering including peripheral nerve. Because MSCs are present in low percentage in the adult BM and also because of some of the disadvantages previously listed, alternative sources have been studied, like the UCT (also called Wharton's jelly). MSCs were defined by the ISCT in 2006, and since that time it is considered that MSCs must adhere to plastic; have a specific profile for the specific surface markers (positive for CD73, CD90, and CD105, and negative for CD14, CD19, CD34, CD45 and HLA-DR). Other important characteristic is that MSCs are also able to undergo tri-lineage differentiation into adipocytes, chondrocytes and osteoblasts^[19]. *In vivo* and *in vitro* studies referred that MSCs have the capacity to induce the regeneration of cartilage, bone,

tendon, and meniscus^[18]. The MSCs are also able to differentiate into neuro-glial cells, which have been studied *in vitro* and *in vivo* using animal models, by our research group^[25]. Children and adult clinical trials have been performed where MSCs were used to treat a wide range of pathologies, including neurological disorders, PNS and CNS injuries (access www.clinicaltrials.gov). In fact, nowadays, the cryopreservation of UCB, and UCT is performed worldwide in private and public cord blood banks. Furthermore, the MSCs from the UCT and hematopoietic stem cells from the UCB have positive clinical outcomes not only in hematologic malignancy patients, where the MSCs work as a co-adjuvant for the hematopoietic transplant success, but also in PNS injuries and neurologic disorders. For that reason, the crucial role of MSCs in tissue renewal and regeneration has been well established for several limiting pathologies, not treated by the traditional therapeutic approaches^[49]. The *in vivo* application of MSCs performed by the authors was intended to improve the regeneration process in the rat sciatic nerve after a neurotmesis injury which was surgically reconstructed using electric conductive tube-guides of PVA-CNTs composition. At that moment there are several nerve tube-guides in the market, however they still have limitations and the functional outcome of the patients is still not complete. In this work the previously developed tube-guides with high electrical conductivity for nerve regeneration (unpublished data) were used *in vivo* using the rat sciatic nerve neurotmesis injury model. A matrix of PVA was used loaded with the following electrical conductive materials: COOH-functionalized multiwall carbon nanotubes (MWCNTs) and PPy PVA-CNTs and PVA-PPy tube, guides, respectively. The tubes production was carried out by a freezing/thawing process (physical cross-linking) and a final annealing treatment. After producing the tube-guides, the physicochemical characterization was performed. The most interesting results were achieved by loading PVA with 0.05% of PPy or COOH-functionalized CNTs, by combining the electrical conductivity of CNTs and PPy with the biocompatibility of PVA matrix, which seems to have potential to be used in peripheral nerve regeneration. For that reason, these two biomaterials were chosen to proceed for *in vivo* pre-clinical trials using the rat sciatic model. As a matter of fact, the microscopic exam performed to lung, heart, kidneys, liver and spleen collected after animal euthanasia, confirmed the absence of inflammation, cell degeneration, necrosis and fibrosis, and no signs of nanotubes, neither carbon deposits were detected in all organs, confirming the biocompatibility of these biomaterials loaded with CNTs. The evaluation of cytocompatibility was performed by measuring the $[Ca^{2+}]_i$ in Fura-2-loaded MSCs cells by using dual wavelength spectrofluorometry, sub-cultured over PVA discs, over PVA loaded with carbon nanotubes (PVA-CNTs) and PVA loaded with PPy (PVA-PPy) discs of 10 mm diameter, as previously described^[3,25,27]. Results correspond to $[Ca^{2+}]_i$ from viable MSCs that did not begin the apoptosis

process, confirming the MSCs ability to expand and viability when associated to PVA, PVA-PPy and PVA-CNTs tube-guides.

The MSCs isolated from the WJ used as cell-based therapy for promoting nerve regeneration when associated to electric conductive tube-guides was previously *in vitro* validated concerning flow cytometry profile, RT-PCR, and cytogenetic analysis. MSCs were expanded to P5-P6 where the culture appeared homogeneous and cells presented their typical fusiform, fibroblast-like, morphology (Figure 1). Also, the flow cytometry analysis confirmed their profile according to ISCT^[19] and the karyotype demonstrated that no structural alterations were present demonstrating absence of neoplastic characteristics in these cells, as well as chromosomal stability to the cell culture procedures. RT-PCR and qPCR targeting specific genes expressed by the MSCs *in vivo* applied was performed to certify that the MSCs used *in vivo* were not differentiated into neuro-glial cells. For the MSCs, the molecular analysis showed a very small amplification of *GFAP* gene, absence of amplification of the *NF-H* and *GAP-43* genes, and reasonable amplification of *NeuN*, β -actin, *GAPDH* and *Nestin* genes, confirming that MSCs used *in vivo* were undifferentiated and not neuro-glial differentiated. In fact, the small detection of the *GFAP* gene expression may be due to the high sensitivity of the molecular tests in comparison with immunocytochemistry tests previously performed using undifferentiated and neuro-glial type differentiated MSCs^[3,18]. Moreover, the expression of the remaining genes, *NeuN*, β -actin, *GAPDH* and *Nestin* was also observed in undifferentiated MSCs. The expression of the housekeeping genes, β -actin and *GAPDH*, is expected to occur. As per the *NeuN* and *Nestin* gene, the observation of its expression in undifferentiated MSCs is not new; Bertani *et al.*^[50] showed that naïve MSCs express at a constitutive level *NeuN* gene, which increases when these cells are chemically induced to differentiate to pre-neuronal cells. Furthermore, compared gene expression profiles before and after MSCs induction for a number of germ layers, and observed that even before neuronal induction, MSCs population and clonal lines expressed a mixture of mesodermal, germinal, endodermal and ectodermal genes, including several whose expression was thought to be restricted to neuronal cells^[51]. Molecular analysis previously performed^[18] on these same genetic markers over the differentiated MSCs showed an increase in the expression of *GFAP*, *NF-H* and *GAP-43* genes. These genes were not expressed, or expressed at very low levels, in the undifferentiated MSCs transcriptome. Overall, these results support the fact that the MSCs used *in vivo* were not differentiated but presented a neuro-glial potential for differentiation confirming previous results where the same MSCs undifferentiated and *in vitro* differentiated into neuro-glial cells were tested in axonotmesis and neurotmesis injuries associated to other biomaterials namely poly(DL-lactide- ϵ -caprolactone), hybrid chitosan and collagen^[3,25,31].

The rat sciatic nerve model has been widely used in experiments on peripheral nerve regeneration and it has been demonstrated that it is reliable and reproducible model, but research on peripheral nerve injury needs to include both functional and morphological analysis^[52]. Since it is not generally agreed which type of evaluation tool is the most useful for evaluation of functional recovery; our research group like others has been using different methods for an overall assessment of nerve function, which has been widely recommended^[53]. The sciatic nerve regeneration after neurotmesis studies described by the authors were followed during 20 wk after the surgical procedure based on the previous experimental work^[17,29,54,55]. The morphological evaluation together with functional data has been used to assess neural regeneration after induced neurotmesis injuries, but some subjective evaluation, depending on the operator/research analysis is observed^[9]. Some methods for evaluation of nerve recovery, like peroxidase and retrograde fluorescent labeling, histomorphometry, and retrograde transport of horseradish^[47,56] fail in assessing the functional recovery, which is essential to evaluate the success of a scaffold application^[57,58]. The present experimental work includes a variety of independent evaluation tools considering the morphologic and functional recovery, in order to understand and estimate the potential therapeutic benefit of a nerve repair strategy^[9]. EPT, WRL, SSI and SFI, have been proven to be valid methods and to give some information to determine functional recovery following sciatic nerve injury, including motor and nociceptive evaluation^[59]. The use of biomechanical techniques and rat's gait kinematic evaluation was a progress in documenting functional recovery, largely published by our research group^[3,9,17,31,33,35]. Indeed, the use of biomechanical parameters allows an accurate analysis of the sciatic denervation/reinnervation process, permitting to understand the integration of the neural control acting on the ankle and foot muscles, and thus allowing to evaluate the nerve and muscle regeneration after neurogenic muscle atrophy associated to neurotmesis injuries^[60,61]. At the end of the 20-wk healing period, it was performed kinematic gait analysis of rats from the groups where it was applied the biomaterial alone or associated to MSCs-based therapies (PVA, PVA-CNTs, PVA-PPy, and PVA-CNTs-MSCs groups) and measures of ankle joint angle at the four selected instants of the stance phase (IC, OT, HR and TO) were obtained (Table 3 and Figure 4). Considering the histological analysis, it was performed stereology of the regenerated sciatic nerves and morphometry analysis of the TA muscles, trying in this way, not only correlate the neurotmesis injury and the secondary neurogenic regional atrophy, but also consider and validate the morphometry of regional muscles (for instance, by biopsy of the injured muscle) as a method to assess functional recovery after peripheral nerve injuries^[18,25]. The restoration of locomotor activity following damage of the PNS has emerged as one of the most important and critical clinical problem in

neuroscience and neurosurgery fields. Regional muscle weakness and impairment of joint control and mobility occurs in many patients with peripheral nerve or spinal cord injuries which results in gait disorders only evaluated with accuracy by kinematics analysis. During the past 10-15 years, experimental work has been carried out on rat gait analysis which may significantly contribute in the future for a more precise peripheral nerve research. Indeed, the use of biomechanical parameters permits an integration of the neural control acting on the ankle and foot muscles, relevant for the analysis of the sciatic denervation/reinnervation effects. The biomechanical analysis is very useful and accurate to evaluate different therapeutic approaches, describing high number of kinematic variables including positions, velocities, and accelerations, often using high speed digital cameras^[35,40,62,63]. There is high variability between individual joint kinematics and between different animals from the same the same experimental group^[64]. The high level of variability observed in normal quadruped walking, affects significantly the precision of joint kinematic measures of functional recovery after nerve injury. It is important to reduce this variability in kinematics analysis to assess functional recovery after neurogenic muscle atrophy and neurotmesis/axonotmesis injuries. One evident advantage is that using a treadmill the operator reduces step-by-step variability in joint kinematics^[59] which has the disadvantage of being expensive equipment. Also the possibility of combining kinematic analysis with other data, such as ground reaction forces, should be consider for a more accurate evaluation of nerve regeneration^[59,64,65]. Our research group has recently analyzed hip, knee and ankle joint kinematics during recovery of rat sciatic nerve axonotmesis injury, using reflective markers attached to the rat hind-limb to track the motion with infra-red capture cameras, to better assess the rat sciatic nerve model hind-limb joint kinematics during walking. Due to physiological constraints and muscle actions it was observed that different joints have different motion patterns within motion planes, more evident when a 3D segmental kinematic analysis using a 3D reconstruction of the rat hind-limb was performed^[9]. This method allowed a more complete segmental kinematic analysis using both planar angles computation (2D) and a 3D reconstruction of the rat hind-limb but unfortunately, in the present experimental work it was only possible to perform a 2D gait analysis^[9]. In the present work, 2D biomechanical analysis (sagittal plan) was carried out applying a two-segment model of the ankle joint, adopted from the model firstly developed by Varejão *et al.*^[40]. For that reason, ankle joint angle values were similar across the experimental groups at the times of IC, OT and HR. However, less acute ankle joint angles observed in PVA-CNTs-MSCs group, compared with PVA-PPy and PVA-CNTs groups might suggest improved ankle muscles function during the push off phase of the rat's gait cycle (Figure 4 and Table 3). It is well known and demonstrated by the scientific bibliography that neuromuscular pathologies

are related to important clinical signs or motor deficits that should be observed, qualified, and quantified, only possible with a precise kinematic analysis^[65,66]. In the field of peripheral nerve research using the rat sciatic nerve model, an improved walking analysis might include several methods combination like joint kinematics, ground reaction forces and electromyographical data of muscle activity. These methods refinements might be important to differentiate the regenerative potential of different scaffolds used, that are not evident when using the traditional standardized methods previously referred^[9,66].

The recent published paper by di Summa *et al.*^[67] where collagen tube-guides (Neurogen[®]) were used *in vivo* to promote peripheral nerve regeneration, combined with schwann cells (SCs), it was possible to demonstrate an improved distal stump sprouting^[68]. This sprouting was more pronounced in the experimental group where the SCs were derived from BM-MSCs when compared to SCs derived from adipose tissue MSCs (AT-MSCs). On the other hand, no significant differences were observed in proximal regeneration among all the experimental groups. BM-MSCs and AT-MSCs -loaded conduits induced a diffuse sprouting pattern of the axons. On the other hand, the tube-guides loaded with SCs induced an enhanced cone pattern and a typical sprouting along the collagen type I conduits walls, showing improved regenerating results. This observation is important and should be related to results obtained from the innervated muscle morphometry analysis. It should be bear in mind that the sprouting is also evaluated and a constant observation in the histomorphometry analysis of the regenerated peripheral nerve after axonotmesis and neurotmesis lesions, where different reconstruction strategies were tested *in vivo* in the rat model by our research group for the past years^[3,25,31,68].

The morphometry and histological analysis of TA muscles collected from rats where the neurotmesis injury was reconstructed with PVA-CNTs-MSCs tube-guides is in fact somehow surprising since in the treatment groups presented in a previous published study (Gärtner *et al.*^[3], 2014), no adverse effect was noticed when MSCs isolated from UC WJ were used. The TA muscles from PVA-CNTs-MSCs group presented the worst results in terms of muscular atrophy after denervation, results not correlated with functional analysis (considering mostly kinematics gait analysis and SSI) (Figure 5). The decreased fiber size observed in these TA muscles was coincident with the smaller sized muscles that were collected at 20 wk, macroscopically evaluated during the collection for histological evaluation. Histologically it was also possible to detect a considerable amount of necrosis with delayed muscle regeneration in this group's TA muscles (Figure 6). Some toxic metabolite resulting from the interaction between the vehicle where the MSCs are suspended (PBS) which has calcium and magnesium, and PVA-CNTs tube-guide, could explain the histological results. These results may occur, not because there is a deleterious effect of the cellular

system, but because the vehicle is not appropriate to the cells microenvironment. As a matter of fact these MSCs were previously tested associated to Floseal® and some local nerve necrosis could be observed by histological analysis. On the other hand, the myelin sheath of the MSCs-treated regenerated nerves was thicker, suggesting that MSCs might exert their positive effects on SCs, the key element in Wallerian degeneration and consequent axonal regeneration^[3]. From the data obtained from the stereology analysis of PVA, PVA-CNTs, PVA-PPy, Graft, End-to-End and PVA-CNTs-MSCs groups, it was also demonstrated a synergistic positive effect on regenerated nerve fibers resulting from combined use of MSCs with the PVA-CNTs tube-guides, where PVA-CNTs-MSCs presented higher myelin thickness (M), ratio myelin thickness/axon diameter (M/d) and ratio axon diameter/fiber diameter (d/D; g-ratio) when compared to PVA, PVA-CNTs, PVA-PPy groups (Table 4). Also, these three stereologic parameters (M, M7d, and g-ratio) measured in PVA-CNTs-MSCs regenerated nerves, were not significantly different from the values obtained from End-to-End and Graft groups. In conclusion, as it was previously reported^[3,25], in the MSCs-based cell therapy applied to neurotmesis nerve injuries, it is observed a significantly higher myelin thickness, and similar to Graft and End-to-End regenerated nerves, which are considered the Gold Standards in nerve neurosurgery. These results clearly are consisted with functional data, from SSI and kinematic gait analysis. The PVA-CNTs and PVA-PPy groups presented significantly higher axon diameters (d) and fiber diameters (D), suggesting also the positive effect of these electric conductive materials on axon regeneration and reestablishment of the neuro-muscular junction in agreement with the TA muscle morphometry analysis.

In conclusion, the results revealed that treatment with MSCs associated to PVA-CNTs tube-guides induced an increased number of regenerated fibers and thickening of the myelin sheet. Functional and kinematics analysis has revealed positive synergistic effects brought by MSCs and PVA-CNTs. The PVA-CNTs and PVA-PPy are promising scaffolds with electric conductive properties, bio and cytocompatible, that might prevent in some degree the secondary neurogenic muscular atrophy by improving the reestablishment of the neuro-muscular junction. Since the present studies were carried out in rats with human MSCs, it is important to continue these studies to evaluate the therapeutic potential of these MSCs in human nerve injuries. However, the results discussed herein show a promising effect of MSCs and PVA-CNTs tube-guides in neurodegenerative diseases that are typified by demyelination since this scaffold induced myelin production in surgically reconstructed nerves after a neurotmesis injury.

COMMENTS

Background

The sought for effective new therapeutic strategies for improving peripheral

nerve regeneration represents one of the hot topics in biomedicine because of the high number of lesions affecting peripheral nerves (much higher than lesions to the spinal cord).

Research frontiers

In this study, the authors have tested *in vitro* and *in vivo* mesenchymal stem cells (MSCs) derived from the umbilical cord matrix [Wharton's jelly (WJ)] associated to electric conductive tube-guides developed by their research group, focusing on its effect in promoting nerve regeneration in the rat neurotmesis model. In particular, *in vivo* assessment of nerve regeneration and functional recovery was carried out using a comprehensive battery of complementary methods of analysis that the authors have developed along their previous experience in the study of nerve repair and regeneration and which include behavioral analysis of motor and nociceptive function, kinematic analysis using high speed cameras and histological analysis of nerve fiber regeneration.

Innovations and breakthroughs

The results of this study open interesting perspectives for the clinical application of biodegradable membranes in peripheral nerve reconstruction associated to MSCs isolated from the umbilical cord matrix. Interestingly, these cells, which are major histocompatibility complex class II negative, not only express both an immune-privileged and immune-modulatory phenotype, but their major histocompatibility complex class I expression levels can also be manipulated, making them a potential cell source for MSC-based therapies. In addition, these cells represent a non controversial source of primitive mesenchymal progenitor cells that can be harvested after birth, cryogenically stored, thawed, and expanded for therapeutic uses.

Applications

The results revealed that polyvinyl alcohol (PVA)-carbon nanotubes (CNTs) and PVA-polypyrrole (PPy) are promising scaffolds with electric conductive properties, bio and cytocompatible, that might prevent in some degree the secondary neurogenic muscular atrophy by improving the reestablishment of the neuro-muscular junction. Also, a promising effect of MSCs and PVA-CNTs tube-guides in promoting myelin production in surgically reconstructed nerves after a neurotmesis injury was demonstrated. A new gateway it therefore opened for using these cells in neurodegenerative diseases that are typified by demyelination.

Terminology

Neurotmesis (in Greek tmesis signifies "to cut") is part of Seddon's classification used to classify nerve damage. It is the most serious nerve injury. In this type of injury, both the nerve and the nerve sheath are disrupted. Nowadays, when a nerve is damaged and there is a neurotmesis injury with a gap, it can be repaired using a nerve tube-guide, whenever it is not possible to perform an end-to-end suture without tension or there isn't a graft available. This work focused on the development of electrical conductive nerve tube-guides, which was achieved by loading PVA with PPy or COOH-functionalized CNTs and their *in vivo* application in the rat sciatic nerve neurotmesis injury model. The inclusion of CNTs and PPy brought a significant increase of electrical conductivity of the simple PVA tube-guide. MSCs as defined by the international society for cellular therapy in 2006, are cells characterized by: (1) their capacity to adhere to plastic; and (2) expression of specific surface markers, namely, CD73, CD90, and CD105, and no expression of CD14, CD19, CD34, CD45 and human leukocyte antigen-DR. Additionally, MSCs are able to undergo tri-lineage differentiation into adipocytes, chondrocytes and osteoblasts.

Peer-review

The article is very interesting. The experimental part is very well designed.

REFERENCES

- 1 **Lundborg G.** Enhancing posttraumatic nerve regeneration. *J Peripher Nerv Syst* 2002; **7**: 139-140 [PMID: 12365560 DOI: 10.1046/j.1529-8027.2002.02019.x]
- 2 **Ribeiro J,** Gartner A, Pereira T, Gomes R, Lopes MA, Gonçalves

- C, Varejão A, Luís AL, Maurício AC. Perspectives of employing mesenchymal stem cells from the Wharton's jelly of the umbilical cord for peripheral nerve repair. *Int Rev Neurobiol* 2013; **108**: 79-120 [PMID: 24083432 DOI: 10.1016/B978-0-12-410499-0.00004-6]
- 3 **Gärtner A**, Pereira T, Armada-da-Silva P, Amado S, Veloso A, Amorim I, Ribeiro J, Santos J, Bácia R, Cruz P, Cruz H, Luís A, Santos J, Geuna S, Maurício A. Effects of umbilical cord tissue mesenchymal stem cells (UCX®) on rat sciatic nerve regeneration after neurotmesis injuries. *J Stem Cells Regen Med* 2014; **10**: 14-26 [PMID: 25075157]
 - 4 **May M**. Trauma to the facial nerve. *Otolaryngol Clin North Am* 1983; **16**: 661-670 [PMID: 6634187]
 - 5 **Fields RD**, Le Beau JM, Longo FM, Ellisman MH. Nerve regeneration through artificial tubular implants. *Prog Neurobiol* 1989; **33**: 87-134 [PMID: 2678271 DOI: 10.1016/0301-0082(89)90036-1]
 - 6 **Meek MF**, Coert JH. Clinical use of nerve conduits in peripheral-nerve repair: review of the literature. *J Reconstr Microsurg* 2002; **18**: 97-109 [PMID: 11823940 DOI: 10.1055/s-2002-19889]
 - 7 **Ghasemi-Mobarakeh L**, Prabhakaran MP, Morshed M, Nasr-Esfahani MH, Baharvand H, Kiani S, Al-Deyab SS, Ramakrishna S. Application of conductive polymers, scaffolds and electrical stimulation for nerve tissue engineering. *J Tissue Eng Regen Med* 2011; **5**: e17-e35 [PMID: 21413155 DOI: 10.1002/term.383]
 - 8 **Jiang X**, Lim SH, Mao HQ, Chew SY. Current applications and future perspectives of artificial nerve conduits. *Exp Neurol* 2010; **223**: 86-101 [PMID: 19769967 DOI: 10.1016/j.expneurol.2009.09.009]
 - 9 **Maurício AC**, Gärtner A, Armada-da-Silva P, Amado S, Pereira T, Veloso AP, Varejão A, Luís AL, Geuna S. Cellular Systems and Biomaterials for Nerve Regeneration in Neurotmesis Injuries. Pignatello R, editor. *Biomaterials Applications for Nanomedicine*, 2011: 978-979 [DOI: 10.5772/24247]
 - 10 **Hudson TW**, Evans GR, Schmidt CE. Engineering strategies for peripheral nerve repair. *Orthop Clin North Am* 2000; **31**: 485-498 [PMID: 10882473 DOI: 10.1016/S0030-5898(05)70166-8]
 - 11 **Schmidt CE**, Leach JB. Neural tissue engineering: strategies for repair and regeneration. *Annu Rev Biomed Eng* 2003; **5**: 293-347 [PMID: 14527315 DOI: 10.1146/annurev.bioeng.5.011303.120731]
 - 12 **George PM**, Saigal R, Lawlor MW, Moore MJ, LaVan DA, Marini RP, Selig M, Makhni M, Burdick JA, Langer R, Kohane DS. Three-dimensional conductive constructs for nerve regeneration. *J Biomed Mater Res A* 2009; **91**: 519-527 [PMID: 18985787 DOI: 10.1002/jbm.a.32226]
 - 13 **Chronakis IS**, Grapenson S, Jakob A. Conductive polypyrrole nanofibers via electrospinning: Electrical and morphological properties. *Polymer* 2006; **47**: 1597-1603 [DOI: 10.1016/j.polymer.2006.01.032]
 - 14 **Baker MI**, Walsh SP, Schwartz Z, Boyan BD. A review of polyvinyl alcohol and its uses in cartilage and orthopedic applications. *J Biomed Mater Res B Appl Biomater* 2012; **100**: 1451-1457 [PMID: 22514196 DOI: 10.1002/jbm.b.32694]
 - 15 **Harun MH**, Saion E, Kassim A, Ekramul Mahmud HNM, Hussain MY, Mustafa IS. Dielectric properties of poly (vinyl alcohol)/ polypyrrole composite polymer films. *JASS* 2009; **1**: 9-16
 - 16 **Ghasemi-Mobarakeh L**, Prabhakaran MP, Morshed M, Nasr-Esfahani MH, Ramakrishna S. Electrical stimulation of nerve cells using conductive nanofibrous scaffolds for nerve tissue engineering. *Tissue Eng Part A* 2009; **15**: 3605-3619 [PMID: 19496678 DOI: 10.1089/ten.tea.2008.0689]
 - 17 **Luís AL**, Rodrigues JM, Geuna S, Amado S, Shirotsaki Y, Lee JM, Fregnan F, Lopes MA, Veloso AP, Ferreira AJ, Santos JD, Armada-Da-silva PA, Varejão AS, Maurício AC. Use of PLGA 90: 10 scaffolds enriched with in vitro-differentiated neural cells for repairing rat sciatic nerve defects. *Tissue Eng Part A* 2008; **14**: 979-993 [PMID: 18447635 DOI: 10.1089/ten.tea.2007.0273]
 - 18 **Pereira T**, Ivanova G, Caseiro AR, Barbosa P, Bártolo PJ, Santos JD, Luís AL, Maurício AC. MSCs conditioned media and umbilical cord blood plasma metabolomics and composition. *PLoS One* 2014; **9**: e113769 [PMID: 25423186 DOI: 10.1371/journal.pone.0113769]
 - 19 **Dominici M**, Le Blanc K, Mueller I, Slaper-Cortenbach I, Marini F, Krause D, Deans R, Keating A, Prockop DJ, Horwitz E. Minimal criteria for defining multipotent mesenchymal stromal cells. The International Society for Cellular Therapy position statement. *Cytotherapy* 2006; **8**: 315-317 [PMID: 16923606 DOI: 10.1080/14653240600855905]
 - 20 **Yang CC**, Shih YH, Ko MH, Hsu SY, Cheng H, Fu YS. Transplantation of human umbilical mesenchymal stem cells from Wharton's jelly after complete transection of the rat spinal cord. *PLoS One* 2008; **3**: e3336 [PMID: 18852872 DOI: 10.1371/journal.pone.0003336]
 - 21 **Weiss ML**, Medicetty S, Bledsoe AR, Rachakatla RS, Choi M, Merchav S, Luo Y, Rao MS, Velagaleti G, Troyer D. Human umbilical cord matrix stem cells: preliminary characterization and effect of transplantation in a rodent model of Parkinson's disease. *Stem Cells* 2006; **24**: 781-792 [PMID: 16223852 DOI: 10.1634/stemcells.2005-0330]
 - 22 **Fu YS**, Cheng YC, Lin MY, Cheng H, Chu PM, Chou SC, Shih YH, Ko MH, Sung MS. Conversion of human umbilical cord mesenchymal stem cells in Wharton's jelly to dopaminergic neurons in vitro: potential therapeutic application for Parkinsonism. *Stem Cells* 2006; **24**: 115-124 [PMID: 16099997 DOI: 10.1634/stemcells.2005-0053]
 - 23 **Shin DH**, Lee E, Hyun JK, Lee SJ, Chang YP, Kim JW, Choi YS, Kwon BS. Growth-associated protein-43 is elevated in the injured rat sciatic nerve after low power laser irradiation. *Neurosci Lett* 2003; **344**: 71-74 [PMID: 12782330 DOI: 10.1016/S0304-3940(03)00354-9]
 - 24 **Carvalho MM**, Teixeira FG, Reis RL, Sousa N, Salgado AJ. Mesenchymal stem cells in the umbilical cord: phenotypic characterization, secretome and applications in central nervous system regenerative medicine. *Curr Stem Cell Res Ther* 2011; **6**: 221-228 [PMID: 21476975 DOI: 10.2174/157488811796575332]
 - 25 **Pereira T**, Gärtner A, Amorim I, Almeida A, Caseiro AR, Armada-da-Silva PA, Amado S, Fregnan F, Varejão AS, Santos JD, Bartolo PJ, Geuna S, Luís AL, Maurício AC. Promoting nerve regeneration in a neurotmesis rat model using poly(DL-lactide-ε-caprolactone) membranes and mesenchymal stem cells from the Wharton's jelly: in vitro and in vivo analysis. *Biomed Res Int* 2014; **2014**: 302659 [PMID: 25121094]
 - 26 **Yoo KH**, Jang IK, Lee MW, Kim HE, Yang MS, Eom Y, Lee JE, Kim YJ, Yang SK, Jung HL, Sung KW, Kim CW, Koo HH. Comparison of immunomodulatory properties of mesenchymal stem cells derived from adult human tissues. *Cell Immunol* 2009; **259**: 150-156 [PMID: 19608159 DOI: 10.1016/j.cellimm.2009.06.010]
 - 27 **Rodrigues JM**, Luís AL, Lobato JV, Pinto MV, Lopes MA, Freitas M, Geuna S, Santos JD, Maurício AC. Determination of the intracellular Ca²⁺ concentration in the N1E-115 neuronal cell line in perspective of its use for peripheral nerve regeneration. *Biomed Mater Eng* 2005; **15**: 455-465 [PMID: 16308461]
 - 28 **Thalhammer JG**, Vladimirova M, Bershadsky B, Strichartz GR. Neurologic evaluation of the rat during sciatic nerve block with lidocaine. *Anesthesiology* 1995; **82**: 1013-1025 [PMID: 7717536 DOI: 10.1097/0000542-199504000-00026]
 - 29 **Amado S**, Rodrigues JM, Luís AL, Armada-da-Silva PA, Vieira M, Gärtner A, Simões MJ, Veloso AP, Fornaro M, Raimondo S, Varejão AS, Geuna S, Maurício AC. Effects of collagen membranes enriched with in vitro-differentiated N1E-115 cells on rat sciatic nerve regeneration after end-to-end repair. *J Neuroeng Rehabil* 2010; **7**: 7 [PMID: 20149260 DOI: 10.1186/1743-0003-7-7]
 - 30 **Koka R**, Hadlock TA. Quantification of functional recovery following rat sciatic nerve transection. *Exp Neurol* 2001; **168**: 192-195 [PMID: 11170734 DOI: 10.1006/exnr.2000.7600]
 - 31 **Gärtner A**, Pereira T, Alves MG, Armada-da-Silva PA, Amorim I, Gomes R, Ribeiro J, França ML, Lopes C, Carvalho RA, Socorro S, Oliveira PF, Porto B, Sousa R, Bombaci A, Ronchi G, Fregnan F, Varejão AS, Luís AL, Geuna S, Maurício AC. Use of poly(DL-lactide-ε-caprolactone) membranes and mesenchymal stem cells from the Wharton's jelly of the umbilical cord for promoting nerve regeneration in axonotmesis: in vitro and in vivo analysis.

- Differentiation* 2012; **84**: 355-365 [PMID: 23142731 DOI: 10.1016/j.diff.2012.10.001]
- 32 **Masters DB**, Berde CB, Dutta SK, Griggs CT, Hu D, Kupsky W, Langer R. Prolonged regional nerve blockade by controlled release of local anesthetic from a biodegradable polymer matrix. *Anesthesiology* 1993; **79**: 340-346 [PMID: 8342843 DOI: 10.1097/0000542-199308000-00020]
- 33 **Amado S**, Simões MJ, Armada da Silva PA, Luis AL, Shirosaki Y, Lopes MA, Santos JD, Fregnan F, Gambarotta G, Raimondo S, Fornaro M, Veloso AP, Varejão AS, Mauricio AC, Geuna S. Use of hybrid chitosan membranes and N1E-115 cells for promoting nerve regeneration in an axonotmesis rat model. *Biomaterials* 2008; **29**: 4409-4419 [PMID: 18723219 DOI: 10.1016/j.biomaterials.2008.07.043]
- 34 **Shir Y**, Zeltser R, Vatine JJ, Carmi G, Belfer I, Zangen A, Overstreet D, Raber P, Seltzer Z. Correlation of intact sensibility and neuropathic pain-related behaviors in eight inbred and outbred rat strains and selection lines. *Pain* 2001; **90**: 75-82 [PMID: 11166972 DOI: 10.1016/S0304-3959(00)00388-2]
- 35 **Varejão AS**, Cabrita AM, Meek MF, Bulas-Cruz J, Melo-Pinto P, Raimondo S, Geuna S, Giacobini-Robecchi MG. Functional and morphological assessment of a standardized rat sciatic nerve crush injury with a non-serrated clamp. *J Neurotrauma* 2004; **21**: 1652-1670 [PMID: 15684656]
- 36 **Varejão AS**, Melo-Pinto P, Meek MF, Filipe VM, Bulas-Cruz J. Methods for the experimental functional assessment of rat sciatic nerve regeneration. *Neurol Res* 2004; **26**: 186-194 [PMID: 15072638 DOI: 10.1179/016164104225013833]
- 37 **Dijkstra JR**, Meek MF, Robinson PH, Gramsbergen A. Methods to evaluate functional nerve recovery in adult rats: walking track analysis, video analysis and the withdrawal reflex. *J Neurosci Methods* 2000; **96**: 89-96 [PMID: 10720672 DOI: 10.1016/S0165-0270(99)00174-0]
- 38 **Bain JR**, Mackinnon SE, Hunter DA. Functional evaluation of complete sciatic, peroneal, and posterior tibial nerve lesions in the rat. *Plast Reconstr Surg* 1989; **83**: 129-138 [PMID: 2909054 DOI: 10.1097/00006534-198901000-00025]
- 39 **Bervar M**. Video analysis of standing--an alternative footprint analysis to assess functional loss following injury to the rat sciatic nerve. *J Neurosci Methods* 2000; **102**: 109-116 [PMID: 11040407 DOI: 10.1016/S0165-0270(00)00281-8]
- 40 **Varejão AS**, Cabrita AM, Meek MF, Bulas-Cruz J, Filipe VM, Gabriel RC, Ferreira AJ, Geuna S, Winter DA. Ankle kinematics to evaluate functional recovery in crushed rat sciatic nerve. *Muscle Nerve* 2003; **27**: 706-714 [PMID: 12766982 DOI: 10.1002/mus.10374]
- 41 **Geuna S**, Gigo-Benato D, Rodrigues Ade C. On sampling and sampling errors in histomorphometry of peripheral nerve fibers. *Microsurgery* 2004; **24**: 72-76 [PMID: 14748030 DOI: 10.1002/micr.10199]
- 42 **Raimondo S**, Fornaro M, Di Scipio F, Ronchi G, Giacobini-Robecchi MG, Geuna S. Chapter 5: Methods and protocols in peripheral nerve regeneration experimental research: part II-morphological techniques. *Int Rev Neurobiol* 2009; **87**: 81-103 [PMID: 19682634 DOI: 10.1016/S0074-7742(09)87005-0]
- 43 **Di Scipio F**, Raimondo S, Tos P, Geuna S. A simple protocol for paraffin-embedded myelin sheath staining with osmium tetroxide for light microscope observation. *Microsc Res Tech* 2008; **71**: 497-502 [PMID: 18320578 DOI: 10.1002/jemt.20577]
- 44 **Geuna S**, Tos P, Battiston B, Guglielmone R. Verification of the two-dimensional disector, a method for the unbiased estimation of density and number of myelinated nerve fibers in peripheral nerves. *Ann Anat* 2000; **182**: 23-34 [PMID: 10668555 DOI: 10.1016/S0940-9602(00)80117-X]
- 45 **Lacerda L**, Ali-Boucetta H, Herrero MA, Pastorin G, Bianco A, Prato M, Kostarelos K. Tissue histology and physiology following intravenous administration of different types of functionalized multiwalled carbon nanotubes. *Nanomedicine (Lond)* 2008; **3**: 149-161 [PMID: 18373422 DOI: 10.2217/17435889.3.2.149]
- 46 **He C**, Yang C, Li Y. Chemical synthesis of coral-like nanowires and nanowire networks of conducting polypyrrole. *Synthetic Metals* 2003; **139**: 539-545 [DOI: 10.1016/S0379-6779(03)00360-6]
- 47 **Mackinnon SE**, Hudson AR, Hunter DA. Histologic assessment of nerve regeneration in the rat. *Plast Reconstr Surg* 1985; **75**: 384-388 [PMID: 2579408 DOI: 10.1097/00006534-198503000-00014]
- 48 **Ronchi G**, Nicolino S, Raimondo S, Tos P, Battiston B, Papalia I, Varejão AS, Giacobini-Robecchi MG, Perroteau I, Geuna S. Functional and morphological assessment of a standardized crush injury of the rat median nerve. *J Neurosci Methods* 2009; **179**: 51-57 [PMID: 19428511 DOI: 10.1016/j.jneumeth.2009.01.011]
- 49 **Parekkadan B**, Milwid JM. Mesenchymal stem cells as therapeutics. *Annu Rev Biomed Eng* 2010; **12**: 87-117 [PMID: 20415588 DOI: 10.1146/annurev-bioeng-070909-105309]
- 50 **Bertani N**, Malatesta P, Volpi G, Sonogo P, Perris R. Neurogenic potential of human mesenchymal stem cells revisited: analysis by immunostaining, time-lapse video and microarray. *J Cell Sci* 2005; **118**: 3925-3936 [PMID: 16091422 DOI: 10.1242/jcs.02511]
- 51 **Woodbury D**, Reynolds K, Black IB. Adult bone marrow stromal stem cells express germline, ectodermal, endodermal, and mesodermal genes prior to neurogenesis. *J Neurosci Res* 2002; **69**: 908-917 [PMID: 12205683 DOI: 10.1002/jnr.10365]
- 52 **Dellon AL**, Mackinnon SE. Selection of the appropriate parameter to measure neural regeneration. *Ann Plast Surg* 1989; **23**: 197-202 [PMID: 2782818 DOI: 10.1097/0000637-198909000-00002]
- 53 **Morris JH**, Hudson AR, Weddell G. A study of degeneration and regeneration in the divided rat sciatic nerve based on electron microscopy. IV. Changes in fascicular microtopography, perineurium and endoneurial fibroblasts. *Z Zellforsch Mikrosk Anat* 1972; **124**: 165-203 [PMID: 5012670 DOI: 10.1007/BF00335678]
- 54 **Luis AL**, Amado S, Geuna S, Rodrigues JM, Simões MJ, Santos JD, Fregnan F, Raimondo S, Veloso AP, Ferreira AJ, Armada-da-Silva PA, Varejão AS, Mauricio AC. Long-term functional and morphological assessment of a standardized rat sciatic nerve crush injury with a non-serrated clamp. *J Neurosci Methods* 2007; **163**: 92-104 [PMID: 17397932 DOI: 10.1016/j.jneumeth.2007.02.017]
- 55 **Simões MJ**, Amado S, Gärtner A, Armada-Da-Silva PA, Raimondo S, Vieira M, Luis AL, Shirosaki Y, Veloso AP, Santos JD, Varejão AS, Geuna S, Mauricio AC. Use of chitosan scaffolds for repairing rat sciatic nerve defects. *Ital J Anat Embryol* 2010; **115**: 190-210 [PMID: 21287974]
- 56 **Mackinnon SE**, Dellon AL. A comparison of nerve regeneration across a sural nerve graft and a vascularized pseudosheath. *J Hand Surg Am* 1988; **13**: 935-942 [PMID: 3225423 DOI: 10.1016/0363-5023(88)90275-4]
- 57 **de Medinaceli L**, Freed WJ, Wyatt RJ. An index of the functional condition of rat sciatic nerve based on measurements made from walking tracks. *Exp Neurol* 1982; **77**: 634-643 [PMID: 7117467 DOI: 10.1016/0014-4886(82)90234-5]
- 58 **Shen N**, Zhu J. Application of sciatic functional index in nerve functional assessment. *Microsurgery* 1995; **16**: 552-555 [PMID: 8538433 DOI: 10.1002/micr.1920160809]
- 59 **Gärtner A**, Pereira T, Gomes R, Luis AL, França ML, Geuna S, Armada-da-Silva P, Mauricio AC. Mesenchymal Stem Cells from Extra-Embryonic Tissues for Tissue Engineering-Regeneration of the Peripheral Nerve. 2013 [DOI: 10.5772/53336]
- 60 **Varejão AS**, Cabrita AM, Geuna S, Melo-Pinto P, Filipe VM, Gramsbergen A, Meek MF. Toe out angle: a functional index for the evaluation of sciatic nerve recovery in the rat model. *Exp Neurol* 2003; **183**: 695-699 [PMID: 14552911]
- 61 **Varejão AS**, Cabrita AM, Meek MF, Bulas-Cruz J, Gabriel RC, Filipe VM, Melo-Pinto P, Winter DA. Motion of the foot and ankle during the stance phase in rats. *Muscle Nerve* 2002; **26**: 630-635 [PMID: 12402284 DOI: 10.1002/mus.10242]
- 62 **Varejão AS**, Cabrita AM, Meek MF, Fornaro M, Geuna S, Giacobini-Robecchi MG. Morphology of nerve fiber regeneration along a biodegradable poly (DLA-epsilon-CL) nerve guide filled with fresh skeletal muscle. *Microsurgery* 2003; **23**: 338-345 [PMID: 12942524 DOI: 10.1002/micr.10147]
- 63 **Costa LM**, Simões MJ, Mauricio AC, Varejão AS. Chapter 7: Methods and protocols in peripheral nerve regeneration experi-

- mental research: part IV-kinematic gait analysis to quantify peripheral nerve regeneration in the rat. *Int Rev Neurobiol* 2009; **87**: 127-139 [PMID: 19682636 DOI: 10.1016/S0074-7742(09)87007-4]
- 64 **Jacobson S**, Guth L. An electrophysiological study of the early stages of peripheral nerve regeneration. *Exp Neurol* 1965; **11**: 48-60 [PMID: 14272559 DOI: 10.1016/0014-4886(65)90022-1]
- 65 **Pereira T**, Gärtner A, Amorim I, Armada-da-Silva P, Gomes R, Pereira C, França ML, Morais DM, Rodrigues MA, Lopes MA, Santos JD, Luis AL, Maurício AC. Biomaterials and Stem Cell Therapies for Injuries Associated to Skeletal Muscular Tissues. 2013 [DOI: 10.5772/5335]
- 66 **Harley BA**, Hastings AZ, Yannas IV, Sannino A. Fabricating tubular scaffolds with a radial pore size gradient by a spinning technique. *Biomaterials* 2006; **27**: 866-874 [PMID: 16118016 DOI: 10.1016/j.biomaterials.2005.07.012]
- 67 **di Summa PG**, Kingham PJ, Campisi CC, Raffoul W, Kalbermatten DF. Collagen (NeuraGen®) nerve conduits and stem cells for peripheral nerve gap repair. *Neurosci Lett* 2014; **572**: 26-31 [PMID: 24792394 DOI: 10.1016/j.neulet.2014.04.029]
- 68 **Gärtner A**, Pereira T, Simões MJ, Armada-da-Silva PA, França ML, Sousa R, Bompasso S, Raimondo S, Shirosaki Y, Nakamura Y, Hayakawa S, Osakah A, Porto B, Luis AL, Varejão AS, Maurício AC. Use of hybrid chitosan membranes and human mesenchymal stem cells from the Wharton jelly of umbilical cord for promoting nerve regeneration in an axonotmesis rat model. *Neural Regen Res* 2012; **7**: 2247-2258 [PMID: 25538746]

P- Reviewer: Aramwit P, Romani A **S- Editor:** Ji FF
L- Editor: A **E- Editor:** Liu SQ





Published by **Baishideng Publishing Group Inc**

8226 Regency Drive, Pleasanton, CA 94588, USA

Telephone: +1-925-223-8242

Fax: +1-925-223-8243

E-mail: bpgoffice@wjgnet.com

Help Desk: <http://www.wjgnet.com/esps/helpdesk.aspx>

<http://www.wjgnet.com>

